Atmospheric Environment 185 (2018) 15–28

Contents lists available at ScienceDirect

Atmospheric Environment

journal homepage: www.elsevier.com/locate/atmosenv

Smoke aerosol chemistry and aging of Siberian biomass burning emissions in a large aerosol chamber

A.-C. Kalogridis[a], O.B. Popovicheva[b], G. Engling[c], E. Diapouli[a], K. Kawamura[d,e], E. Tachibana[e], K. Ono[e], V.S. Kozlov[f], K. Eleftheriadis[a,*]

[a] ERL, Institute of Nuclear and Radiological Science & Technology, Energy & Safety N.C.S.R. "Demokritos", 15310 Athens, Greece
[b] Skobeltsyn Institute of Nuclear Physics, Moscow State University, Moscow, Russian Federation
[c] Department of Biomedical Engineering & Environmental Sciences, National Tsing Hua University, Hsinchu, Taiwan, ROC
[d] Chubu Institute for Advanced Studies, Chubu University, Kasugai 487-8501, Japan
[e] Institute of Low Temperature Science, Hokkaido University, Sapporo, Japan
[f] Zuev Institute of Atmospheric Optics, Siberian Branch Russian Academy of Sciences, Tomsk, Russian Federation

ARTICLE INFO

Keywords:
Biomass burning
Chamber experiments
Aerosol emission factors
Aging in dark conditions
Anhydrosugars
Dicarboxylic acids

ABSTRACT

Vegetation open fires constitute a significant source of particulate pollutants on a global scale and play an important role in both atmospheric chemistry and climate change. To better understand the emission and aging characteristics of smoke aerosols, we performed small-scale fire experiments using the Large Aerosol Chamber (LAC, 1800 m^3) with a focus on biomass burning from Siberian boreal coniferous forests. A series of burn experiments were conducted with typical Siberian biomass (pine and debris), simulating separately different combustion conditions, namely, flaming, smoldering and mixed phase.

Following smoke emission and dispersion in the combustion chamber, we investigated aging of aerosols under dark conditions. Here, we present experimental data on emission factors of total, elemental and organic carbon, as well as individual organic compounds, such as anhydrosugars, phenolic and dicarboxylic acids. We found that total carbon accounts for up to 80% of the fine mode ($PM_{2.5}$) smoke aerosol. Higher $PM_{2.5}$ emission factors were observed in the smoldering compared to flaming phase and in pine compared to debris smoldering phase. For low-temperature combustion, organic carbon (OC) contributed to more than 90% of total carbon, whereas elemental carbon (EC) dominated the aerosol composition in flaming burns with a 60–70% contribution to the total carbon mass. For all smoldering burns, levoglucosan (LG), a cellulose decomposition product, was the most abundant organic species (average LG/OC = 0.26 for pine smoldering), followed by its isomer mannosan or dehydroabietic acid (DA), an important constituent of conifer resin (DA/OC = 0.033). A levoglucosan-to-mannosan ratio of about 3 was observed, which is consistent with ratios reported for coniferous biomass and more generally softwood.

The rates of aerosol removal for OC and individual organic compounds were investigated during aging in the chamber in terms of mass concentration loss rates over time under dark conditions and compared to the loss rate of EC. The latter is used as an inert tracer for estimating aerosol mechanical deposition and wall losses of the otherwise chemically conserved aerosol species. The OC/EC ratio increased with smoke aging for the flaming phase, suggesting a production/partitioning of organic compounds after emission. On the other hand, for smoldering burns OC/EC ratios decreased further with aging due to additional sinks of OC, other than those related to deposition and wall losses alone, such as evaporation of semi-volatile compounds. The chemical fingerprints of the major PM components of fresh and aged smoke found in this study are proposed to be used for the assessment of contributions from Siberian biomass burning to atmospheric pollution in source apportionment studies like those using molecular marker approaches.

1. Introduction

Biomass burning is known to be a major contributor to the global budget of aerosols (Amiridis et al., 2012; Bond et al., 2013; Kasischke and Penner, 2004). It releases into the atmosphere particulate species such as black carbon (BC) and organic carbon (OC), and it is considered

* Corresponding author.
E-mail address: elefther@ipta.demokritos.gr (K. Eleftheriadis).

https://doi.org/10.1016/j.atmosenv.2018.04.033
Received 1 December 2017; Received in revised form 6 April 2018; Accepted 22 April 2018
Available online 23 April 2018
1352-2310/ © 2018 Elsevier Ltd. All rights reserved.

an important contributor to radiative forcing of climate. Arctic climate is especially BC-sensitive because of the impact of its deposition on snow, accelerating the icecap melting and changing the surface albedo (AMAP, 2012). The direct and indirect impacts of BC aerosols induce the highest uncertainty amongst climate active species with respect to temperature changes, radiative forcing, and cloud formation (Boucher et al., 2013; Koch et al., 2009; Popovicheva, 2010).

Siberia is one of the world's major boreal forest fire areas (Damoah et al., 2004; Lee et al., 2005; Stocks et al., 1998). Smoke pollution plumes from Siberian forest fires can be transported over hundreds of kilometers, often approaching the Arctic coast at approximately 70 °N (Paris et al., 2009), as well as southwards towards the Mediterranean sea (Diapouli et al., 2014), and have been identified as a major source of climate-relevant species emitted at northern latitudes (Lavoué et al., 2000). Significant contribution to springtime Arctic aerosols from fires in Russia was demonstrated when biomass burning (BB) plumes increased the atmospheric burden of BC and OC 2.6 times above the Arctic Haze background (Warneke et al., 2009). Long-range transport of Siberian BB has significantly influenced the chemical composition of carbonaceous aerosols globally: in the western North Pacific rim (Agarwal et al., 2010) and North East Greenland (Nguyen et al., 2013).

Physico-chemical characteristics of BB aerosols are highly variable. Much of the variance in the particle emissions and chemical composition is due to the phase of burning (that is, flaming versus smoldering) and the ecosystem characteristics (type of biomass, fuel moisture, soil properties, temperature, etc.) (Reid et al., 2005). Slow and low-temperature smoldering fires (flameless form of combustion) yield a substantially higher conversion of a fuel to toxic compounds than does flaming combustion (Alves et al., 2016; McKenzie et al., 1995; Morawska and (Jim) Zhang, 2002). Such fires produce brown carbon (BrC) that consists largely of weakly light-absorbing resinous organic carbon aerosols (Popovicheva et al., 2017). Increasing the oxygen supply leads to higher temperatures and flaming combustion, which produces particulate matter (PM) with a lower OC and higher BC content, the latter being a strongly light-absorbing component. Regional smoke plumes result from numerous mixed phase fires where the relative amount of flaming versus smoldering burns is poorly characterized. Due to the mixing of these two different types of thermal decomposition, the climatic impact of biomass burning remains rather uncertain.

Despite concerns about the climatic impact and environmental hazards related to millions of tons of PM emitted by wildfires, observations of aerosol chemical composition and BC in Siberia have been reported for a limited number of sites (Kozlov et al., 2008; Kuokka et al., 2007; Paris et al., 2009). During forest fire episodes, most of the aerosol mass appears to consist of organic particulate matter with high concentrations of BB markers such as levoglucosan, oxalate and potassium (Kuokka et al., 2007). A few measurement campaigns during experimental fires were undertaken to address sub-Arctic boreal forest fire emissions (Samsonov et al., 2012). According to their findings, the mass of total emitted PM represented about 1–7% of consumed biomass, and consisted to 77% of organic substances, 8% of elemental carbon (EC), and 6% of inorganic species.

The OC fraction of biomass burning aerosols is dominated by carbohydrates (Reid et al., 2005). Among them, some monosaccharides, which are the simplest carbohydrates in that they cannot be hydrolyzed to smaller carbohydrates, have been identified as molecular markers of biomass burning (Puxbaum et al., 2007; Simoneit et al., 1999; Ward et al., 2006). This is the case of anhydrosugars (levoglucosan and its stereoisomers mannosan and galactosan) which are present in combustion products from biomass containing cellulose and hemicellulose and which tend to be adsorbed to aerosols because of their low volatility (Kirchgeorg et al., 2014; Simoneit et al., 1999). Other compounds, such as phenolic acids, which are lignin breakdown products, have also been used as proxy for biomass burning (Alves et al., 2010). Moreover, dehydroabietic acid is a product of the thermal decomposition of diterpenoids, which are important biomarker constituents of conifer resins (Oros and Simoneit, 2001b). Simoneit et al. (1999) reported that the burning of Douglas fir, Lodgepole pine, Ponderosa pine, Sitka spruce and Western white pine emit more dehydroabietic acid than levoglucosan. Thus, this resin acid has been proposed as a potential molecular marker specifically for combustion of Gymnosperm (conifers) (Alves et al., 2016; Simoneit et al., 1999, 2000). Aliphatic diacids, (from C_2 to C_{10}), unsaturated diacids, ω-oxocarboxylic acids and α-dicarbonyls are also products of biomass burning (Kawamura et al., 2013; Kawamura and Bikkina, 2016). While these acids have been measured in ambient air in many different places (including some areas dominated by certain emission sources), there have been few source emission (e.g., chamber) measurements. Therefore, it is of interest to quantify these species under controlled combustion conditions. Many trace elements, mostly alkali earth metals (carbonates), dominate the inorganic fraction in fly ash with large impact of soil evolving by intensive fires (Kavouras et al., 2012; Popovicheva et al., 2016a). Water-soluble ions (potassium, halides, sulfates) are also produced by decomposition of biomass and subsequent condensation in the smoke plume.

Following emission, smoke particles are subject to physico-chemical processes in the plume that can alter their properties. Dynamic changes in particle concentration and size may increase aerosol mass loadings in the smoke plume, and heterogeneous reactions in humid conditions produce more water-soluble inorganic salts (Li et al., 2015). Additionally, secondary organic aerosol (SOA) formation in the smoke plume can occur, while it becomes significant especially when solar radiation can induce photochemical reactions (Popovicheva et al., 2014; Reid et al., 2005; Tiitta et al., 2016). These changes in the particle properties can alter the direct and indirect effects of BB, impacting single scattering albedo and hygroscopicity.

In view of the difficulty of accounting for all the variability in particle emissions from natural biomass fires, combustion chamber experiments have been performed allowing for measurement of fire-integrated smoke properties from a single fuel type under conditions simulating the entire burning process, i.e., from ignition to smoldering through flaming. In the Fire Lab at Missoula Experiments (FLAME), a series of open biomass burning experiments were performed to derive emission factors of PM for 33 different plant materials that are frequently consumed by wildfires in the U.S (Carrico et al., 2010; Engling et al., 2006b; Hosseini et al., 2010; Levin et al., 2010; McMeeking et al., 2009). A detailed chemical characterization of particle emissions from the combustion of European conifer species, savannah grass, African hardwood, and German and Indonesian peat has also been performed by Iinuma et al. (2007). Such studies were lacking for typical Siberian closed-canopy coniferous forest biomass, despite the frequency and intensity of forest fires in this region and the environmental hazards related to the impact on Arctic climate.

In that context and to fill the gaps in available data on particulate emissions and smoke chemistry of fires specific to the Siberian boreal region, typical Siberian biomass (pine and debris) were burned in the Large Aerosol Chamber (LAC) of the Institute of Atmospheric Optics Russian Academy of Sciences (Tomsk, Siberia). The originality of our approach resides in the fact that experiments were conducted under controlled combustion conditions to simulate separately flaming, smoldering and mixed burning phases. A comprehensive optical and microstructural analysis showed that the temperature regime of combustion plays a key role in the formation and time evolution of smoke (Popovicheva et al., 2015). Smoldering fires produced particles with high OC while flaming fires produced a high EC content and soot agglomerates. Individual particle analysis of smoke microstructure was used to apportion the particles into major characteristic groups: Soot and Organic, which accounted for about 90% and 60% of total particle numbers emitted from the flaming and smoldering fires, respectively. Extended individual particle analyses also revealed the hygroscopicity of smoke aerosol (Popovicheva et al., 2016b).

Studies in the LAC, as well as in the other combustion chambers mentioned above, were performed in dark conditions. Simulating sunlight source in the combustion chamber has the advantage of enabling the study of photochemical aging. In a few smog chamber studies, this was done by exposing the diluted emission plume to UV light (Grieshop et al., 2009; Hennigan et al., 2010, 2011; Hoffmann et al., 2010). Still, simulations of small-scale fires under controlled combustion conditions in the dark provide us with fundamental knowledge about the processes, smoke characteristics and aging in the atmosphere at night time (Li et al., 2015).

Here, we continue studies in the Large Aerosol Chamber and focus on the comprehensive characterization of chemical composition of smoke aerosols under well-controlled combustion conditions. Total carbon, OC, EC, and selected organic molecular markers including dicarboxylic acids, oxoacids, α-dicarbonyls and related compounds in PM_{10} and $PM_{2.5}$ samples were measured in flaming, smoldering and mixed phases. Emission ratios (related to OC) as well as emission factors (related to fuel consumed) from small-scale fires of Siberian forest pine wood and debris are determined. Furthermore, aging of smoke particles following the emission is investigated in order to assess the transformation of the aerosol chemical properties under dark conditions.

2. Methods

2.1. Experimental fires

Small-scale fires were conducted in the Large Aerosol Chamber (LAC), an isolated hermetically tight oblong chamber of a total volume of 1800 m^3 (25 m length, 10 m diameter). The inside walls were covered by thermo-isolated material of 15 cm thickness for maintaining an internal temperature independent of external conditions. One main advantage of the LAC chamber is that wall losses are minimized due to its very large volume. Indeed, large chambers reduce chamber surface area-to-volume ratios, thereby minimizing wall effects such as removal of gas-phase species and deposition of particles on the wall of the chamber (Cocker et al., 2001). A detailed description of the combustion chamber is given in Popovicheva et al. (2015).

The fuels used were Scots pine wood (*Pinus sylvestris* L.) and debris (mixture of pine needles, branches, cones), which are common wildland biomass from Siberian boreal coniferous forests. Fire experiments were designed to simulate individual combustion events that proceed from ignition through flaming or smoldering combustion. One oven (8 L volume) was used to simulate low temperature combustion. Smoldering was achieved by igniting the fuel when temperatures were approaching 400 °C and was maintained by limiting excess oxygen, while visually ensuring absence of open flames. In a second oven (5 L volume), flaming was conducted by igniting the fire at a temperature approaching 700 °C. In order to better represent wildfires characterized by a changing flaming and smoldering processes, mixed combustion phase was also simulated. To this end, both ovens were used simultaneously for burning one half of total mass of a given fuel in smoldering and the other half in flaming phase. This approach has a strong advantage; it allows distinguishing the burning conditions, removing the uncertainties resulting from fire-integrated smoke interpretation and studying independently the impact of the combustion phase on smoke aerosol properties.

200-400 g of fuel was used in each controlled burn. Both types of biomass had been stored indoor. A fuel moisture content of 12.4% of mass for debris and 6.8% for pine wood were achieved, representing wildfire fuel moisture during drought episodes. Fuel moisture was determined by heating a fuel sample at 100 °C and measuring the mass loss.

The smoke from each burn was allowed to fill the chamber and remained there for a period of 48 h, in order to study the smoke time evolution. Upon entering the chamber, the smoke was rapidly diluted and cooled to room-air temperatures, i.e., 20–23 °C. Relative humidity of the air inside the LAC remained relatively constant, in the range of 20–40%, during the whole combustion experiment. After uniform filling. i.e., within 2 h, the dilution ratio of the smoke inside the chamber relative to the smoke inside the ovens was between 1.4×10^5-3.6×10^5, consistent with highly diluted conditions as found in ambient plumes downwind of a point source (Donahue et al., 2006). Initial particle mass concentrations inside the chamber ranged between 4000 and 20,000 μg m^{-3} depending on the type and mass of fuel used and the combustion temperature.

2.2. Sampling

Distinction between coarse and fine PM fractions is of fundamental importance because it reflects differences in the nature, origin, and environmental fate of aerosols. In order to separate fine and coarse particles, two sampling inlets (Digitel, CH) for sampling particulate matter with aerodynamic diameters less than 10 (PM_{10}) and 2.5 μm ($PM_{2.5}$) were used for each burn. The sampling line consisted of 2-m long stainless steel tube, whose inner diameter was 25 mm. $PM_{2.5}/PM_{10}$ inlets were extended horizontally at a distance of 2.5 m from the chamber wall towards the central part of the chamber. Particles were collected at a stable flow rate of 1 $m^3 h^{-1}$. For some burns, total suspended particles (TSP) were collected instead of PM_{10}. Aerosol was collected on quartz fiber filters (Pallflex, 47 mm) for the quantification of OC, EC and total carbon (TC = OC + EC), as well as individual organic compounds.

After ignition of biomass, aerosol scattering, which is related to smoke particle mass concentration (Kozlov et al., 2014), was steadily rising and reached maximum values typically within 2 h. At this time, smoke had homogeneously filled the chamber and the first sampling operation begun. Smoke particles collected at this point were termed as “fresh”. To evaluate the time evolution of “aged” smoke, additional sampling was performed 24 h and 48 h after fire ignition, when the smoke mass concentration in the chamber had significantly decreased. Filter loading was controlled by visual inspection in order to obtain a light-grey color. Based on gravimetric measurements, filter loadings were estimated at approximately 1 μg of particle mass. Depending on conditions, sampling time varied between 2 min and 1 h.

The chamber remained closed without light exposure during smoke evolution. Outside air was conditioned for temperature and humidity and pumped into the chamber prior to each burn. Samples were stored in a refrigerator and analyzed *a posteriori* in a chemical laboratory.

In total, six different combinations of combustion phases and biomass types were performed, and for most of them several replicates were performed in order to investigate the burn-to-burn variability of the combustion process (Table 1). Two filters for $PM_{2.5}$ and two filters for PM_{10} (or TSP) were collected during the 2nd, 24th and 48th hour of each experiment. The first filters were used for EC/OC measurements, while different punches from the second ones were used for the different chemical analysis. In total, about 100 filters were collected.

2.3. Analytical methods

2.3.1. EC/OC/TC

Organic carbon (OC) and elemental carbon (EC) concentrations were determined on quartz fibre filters by thermal–optical transmittance (TOT) method, using a Lab OC-EC Aerosol Analyzer (Sunset Laboratory, Inc.). A NIOSH-like protocol with a maximum temperature of 840 °C in the He-mode was applied (Peterson and Richards, 2002). A comparative analysis of the three most widely used protocols, NIOSH, EUSAAR2 (Cavalli et al., 2010) and IMPROVE_A (Chow et al., 2007), was performed on a subset of 12 filters. As illustrated in Fig. 1, good agreement of the OC and EC concentrations measured by the different protocols was observed, confirming the suitability of the NIOSH protocol for the determination of the EC/OC content of the studied biomass

Table 1
Combinations of combustion phase and biomass in LAC burns.

No	Type of burning phase	Biomass	Replicates	Sampling time (hours after ignition)[a]
1	Smoldering (400 °C)	Pine	a	2, 24, 48
			b	2
			c	2, 24
2	Flaming (700 °C)	Pine	a	2
			b	2, 24, 48
			c	2
3	Mixed (700 °C & 400 °C)	Pine	a	2, 24, 48
			b	2
			c	2
4	Smoldering (400 °C)	Debris	a	2
			b	2
			c	2, 24, 48
			d	2
6	Flaming (700 °C)	Debris	a	2
			b	2
			c	2
			d	2

[a] Hours after ignition: 2-h: fresh, 24- and 48-h: aged.

burning samples.

2.3.2. Carbohydrates

Quantification of selected carbohydrates, namely, levoglucosan, mannosan, galactosan, as well as mannitol and arabitol was performed. Sample preparation for measurement included the extraction of a punch (2.2 cm^2) of each quartz filter with 3.0 mL ultra-pure deionized water (> 18.2 MΩ resistivity) under ultrasonic agitation for 60 min. The aqueous extracts were filtrated through Teflon syringe filters (0.45 μm pore size) to remove insoluble materials including quartz filter debris. The extract solutions were stored at 4 °C until sample analysis. Carbohydrates were quantified by high-performance anion exchange chromatography with pulsed amperometric detection (HPAEC-PAD) on a Dionex ICS-3000 system (Dionex, Sunnyvale, CA, USA). Separation of the individual carbohydrate species was achieved with a Dionex CarboPac MA1 analytical column preceded by a CarboPac MA1 guard column with an aqueous sodium hydroxide (NaOH, 480 mM) eluent at a flow rate of 0.4 mL min^{-1}. All carbohydrates were below detection limits in blank samples. Additional information about the HPAEC-PAD method can be found elsewhere (Iinuma et al., 2009).

2.3.3. GC-FID speciation

Filter samples were analyzed for a series of dicarboxylic acids, oxocarboxylic acids and α-dicarbonyls (Table 2) using a capillary gas chromatograph (GC) equipped with a flame ionization detector (FID) following the techniques of (Kawamura and Ikushima, 1993) and (Kawamura, 1993). First, an aliquot of filters was extracted with organic-free pure water (5 mL x 3) and the extracts were adjusted to pH = 8.5–9.0 using 0.05 M KOH solution and then concentrated to dryness using a rotary evaporator under vacuum and nitrogen blow down system (Deshmukh et al., 2016). The extracts were then derivatized with 14% BF_3 in n-butanol to convert carboxyl groups to butyl esters and oxo and aldehyde groups to dibutoxy acetals. The derivatives were finally dissolved in n-hexane and injected into a capillary gas chromatograph equipped with flame ionization detector (GC-FID) for the determination. The GC was equipped with a split/splitless injector and HP-5 fused silica capillary column (Kawamura et al., 2013). The uncertainties of the GC-FID determination for the major species were ± 10%. The data reported here were corrected for laboratory blanks.

2.3.4. GC-MS analysis

For the analyses of additional polar organic compounds, such as some organic acids, an aliquot of the filter samples was extracted with a mixture (10 mL) of dichloromethane and methanol (2:1). After the concentration, the extracts were reacted with 50 μL of N,O-bis-(trimethylsilyl)trifluoroacetamide (BSTFA) with 1% trimethylsilyl chloride and 10 μL of pyridine for 3 h at 70 °C to convert OH groups to trimethylsilyl (TMS) ethers and carboxylic acids to TMS esters. After the reaction, the derivatives were diluted by the addition of 140 μL of n-hexane containing internal standard (C13 n-alkane, 1.43 ng μL^{-1}) prior to the determination by gas chromatography-mass spectrometry (GC-MS). GC-MS analyses of the derivatized fraction were performed on a Hewlett-Packard model 6890 GC coupled to a Hewlett-Packard model 5973 MSD. The GC was equipped with a split/splitless injector and a DB-5ms fused silica capillary column (30 m × 0.25 mm i.d., 0.25 μm film thickness). The GC oven temperature was programmed from 50 °C (2 min) to 120 °C at 15 °C min^{-1} and then to 300 °C at 5 °C min^{-1} with a final isothermal hold at 300 °C for 16 min. The MS was operated in the electron impact ionization (EI) mode at 70 eV and scanned from 50 to 650 Da. Data were acquired and processed with the Chemstation software. For more details, please see Simoneit et al. (2004) and Fu et al. (2008).

2.4. Emission ratios and emission factors calculation

Absolute concentrations in smoke plumes represent the degree of dilution of combustion products in ambient air. Therefore, emission ratios and emission factors have been calculated for all particulate species measured. Emission ratios (ER) relate the emission of any specie X to that of a reference specie, such as organic carbon (OC) (McMeeking et al., 2009):

$$ER(X) = \frac{[X]}{[OC]} \quad (1)$$

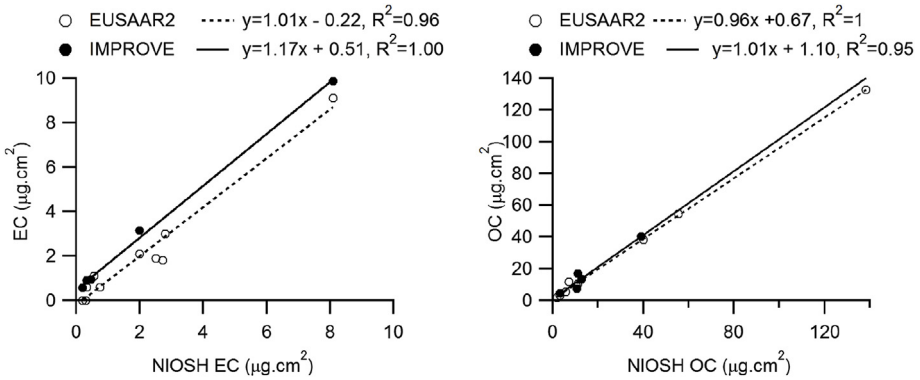

Fig. 1. Scatter plots and regression analysis of EUSAAR2 (empty circles) and IMPROVE_A (black circles) protocols against the NIOSH protocol, for EC (left) and OC (right) measurements by thermal–optical transmittance (TOT) method performed on a subset of 12 filters.

Table 2
List and abbreviations of dicarboxylic acids, keto-carboxylic acids and alpha-dicarbonyls measured.

DI-CARBOXYLIC ACIDS							
Saturated n-dicarboxylic acids		Branched dicarboxylic acids		Unsaturated dicarboxylic acids		Oxodicarboxylic acids	
C_2	oxalic	iC_4	methylmalonic	M	maleic	hC_4	malic
C_3	malonic	iC_5	methylsuccinic	F	fumaric	kC_3	ketomalonic
C_4	succinic	iC_6	2-ethylglutaric	mM	methylmaleic	kC_7	ketopimelic
C_5	glutaric			Ph	phthalic		
C_6	adipic			iPh	isophthalic		
C_7	pimelic			tPh	terephthalic		
C_8	sebacic						
C_9	azelaic						
C_{10}	decanedioic						
C_{11}	undecanedioic						
C_{12}	dodecanedioic						
KETO-CARBOXYLIC ACIDS							
$C_{2\omega}$	2-oxoethanoic (glyoxylic)						
$C_{3\omega}$	3-Oxopropanoic						
$C_{4\omega}$	4-oxobutanoic						
$C_{5\omega}$	5-oxopentanoic						
$C_{7\omega}$	7-oxoheptanoic						
$C_{8\omega}$	8-oxooctanoic						
$C_{9\omega}$	9-oxononanoic						
Pyr	pyruvic						
α-DICARBONYLS							
Gly	glyoxal						
MeGly	methylglyoxal						

The emission ratio is a very useful and critical parameter for any trace compound from BB, since it enables the comparison between laboratory-based measurements and can be applied for estimating BB contributions in field observations.

In our study, the emission factor EF(X) of each measured compound X, expressed in g kg^{-1}, represents the quantity emitted per unit of fuel dry mass. We calculated the mass of aerosol species emitted during the chamber burns by multiplying mass concentrations [*X*], expressed in g m^{-3}, determined from filter measurements by the total volume of the chamber ($V_{chamber}$, in m^3). This approach assumes that smoke is well dispersed and is homogeneously filling the chamber. It is then possible to calculate the emission factor, knowning the fuel dry mass ($M_{dry\ fuel}$) burned, as:

$$EF(X) = \frac{[X] \times V_{chamber}}{M_{dry fuel}} \quad (2)$$

2.5. Reconstruction of PM concentrations

Total $PM_{2.5}$ mass concentrations in chamber simulations were computed by summing the mass concentration of EC, organic matter (OM) and inorganic species.

$$PM_{2.5}(estimated) = EC + OM + \sum inorganic\ species \quad (3)$$

The concentration of particulate OM was estimated by multiplying the measured concentration of OC by a conversion factor *f* accounting for associated O, H, N and other elements, from the C mass concentrations attributed to OC. This factor, which is an estimate of the average molecular weight per carbon weight for the organic aerosol exhibits a great variability depending on conditions of emission and atmospheric transformation. Values within the range of 1.4–1.8 have been suggested for biomass burning aerosols by Reid et al. (2005), whereas Turpin and Lim (2001) found that values below 1.4 are likely non-realistic and recommend values as high as 2 for wood smoke aerosols. Here, a conversion factor of 2 was therefore used to compute the total organic mass concentration. From indicative ion chromatography analysis, inorganic species were found to represent 1–5% of $PM_{2.5}$ mass. Bearing in mind the uncertainties related to the *f* factor, reconstructed PM emission factors, EF($PM_{2.5}$) and EF(PM_{10}) have to be considered here as an approximation.

3. Results & Discussion

3.1. Fresh smoke emissions

3.1.1. Particulate mass emissions

$PM_{2.5}/PM_{\mathbf{10}}$ ratios (where $PM_{\mathbf{10}}$ = PM_{10} or TSP) range between 0.8 and 1 (Table 3), confirming that total aerosol mass is dominated by particles in the sub-2.5 μm diameter size range, as reported previously for other biomass burning emissions (Kleeman et al., 1999; McMeeking et al., 2009; Ward and Hardy, 1991). Averaged emission factors over a few replicates for reconstructed $PM_{2.5}$ and $PM_{2.5}/PM_{10}$ ratios are presented in Table 3. EF(PM_{10}) and EF($PM_{2.5}$) range from 15 to 75 and 9–61 g kg_{fuel}^{-1}, respectively, depending on the burning phase and type of fuel. Highest emission factors of PM_x (where X = 10, 2.5) are observed for the Pine/Smoldering combination, whereas the lowest emission factors are observed for the Debris/Flaming one. For pine, EF (PM_X) in the smoldering phase are on average 5 times higher than in the

Table 3
Average (± standard deviation) emission factors (g $kgfuel^{-1}$) for $PM_{2.5}$, EC, OC and TC, as well as $PM_{2.5}/PM_{10}$, OC/EC, and OC/TC ratios for each fuel/burning phase combination.

Fuel/burning phase	$PM_{2.5}$	EC	OC	TC	$PM_{2.5}/PM_{10}$	OC/EC	OC/TC
Debris Smoldering	9.10 ± *1.6*	< 0.1 ± *0.1*	4.1 ± 0.4	4.1 ± 0.4	0.6	93.6 ± 21.4	1.0 ± 0.0
Debris Flaming	12.0 ± *1.8*	6.1 ± *1.7*	3.3 ± 0.6	9.4 ± 2.0	0.9	0.6 ± 0.1	0.4 ± 0.1
Pine Smoldering	60.7 ± *4.6*	0.1 ± *0.0*	28.7 ± 1.5	28.9 ± 1.5	0.8	203.2 ± 5.8	1.0 ± 0.0
Pine Flaming	12.3 ± *4.0*	6.9 ± *2.2*	3.3 ± 2.7	10.2 ± 4.1	0.8	0.5 ± 0.3	0.3 ± 0.1

flaming phase, reflecting the difference in combustion efficiency. EF (PM_x) are less diverse between smoldering vs flaming phases when burning debris. Our results are in agreement with precedent studies reporting an increase in the $PM_{2.5}$ emission factor with decreasing combustion efficiency, that is with increasing relative amounts of smoldering combustion (McMeeking et al., 2009; Reid et al., 2005; Zepp et al., 1992). Based on a literature review of biomass burning emissions, including a large number of plant species and ecosystems (boreal, temperate and some tropical forests) and from measurements in a variety of environments (from laboratory burns, ground-based fire towers, and aircraft measurements), Reid et al. (2005) estimated average fine aerosol emission factors of about 9 and 34 g kg_{fuel}^{-1}, respectively, for flaming and smoldering combustion measurements, with relative standard deviations higher than 75%. This high variability has been attributed to the combination of different factors such as fuel type/characteristics, fire size/intensity and sampling bias. From the open combustion of different plant species during a series of controlled laboratory burns during the FLAME experiment, emission factors were also calculated for 33 different types of plant material (McMeeking et al., 2009). Average EF($PM_{2.5}$) over various biomass species were 18 and 68 g kg_{fuel}^{-1} in flaming and smoldering phases, respectively, which is in agreement with the differences found in our experiments, reflecting the respective combustion efficiencies. Experimental fires were also conducted in boreal forests of pine and larch mixed wood in central Siberia in order to quantify particulate emissions from sub-Arctic fires burning (Samsonov et al., 2012). According to these findings, EF($PM_{2.5}$) ranged between 10-30 and 10–70% g kg_{fuel}^{-1} during flaming and smoldering forest fires, respectively.

3.1.2. Carbonaceous fractions

Ratios of OC (as well as EC and TC) in $PM_{2.5}$ versus in PM_{10} termed as $OC_{(PM2.5)}/OC_{(PM10)}$ (similarly for EC and TC) are illustrated in Fig. 2.

The graph represents the average and standard deviation values for all burns performed in smoldering and flaming phases, independently of the type of fuel used. The ratio between OC (as well as EC and TC) in $PM_{2.5}$ and PM_{10} typically varies between 0.8 and 1. This suggests no significant differences between the carbon fraction composition of the fine and coarse aerosols for smoldering and flaming burns. In view of these results, only $PM_{2.5}$ measurements will be reported for the carbon fractions in the following discussion.

Varying EF (TC) and OC/EC ratios are observed depending on the combustion phase and type of fuel burned (Fig. 3).

When burning pine, TC emission factors range between 25 and 40 g kg_{fuel}^{-1} in the smoldering phase, while flaming phase results are 2–5 fold lower. EF (TC) for pine is higher than for debris. Also, while burning debris, no significant differences are observed for different combustion phases.

For low-temperature combustion, PM is dominated by OC. Under

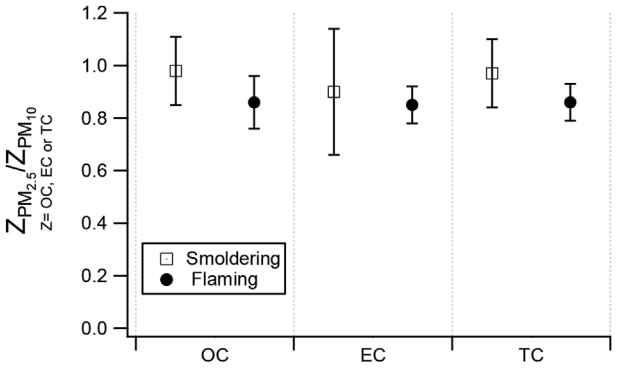

Fig. 2. Average $OC_{(PM2.5)}/OC_{(PM10)}$, $EC_{(PM2.5)}/EC_{(PM10)}$, and $TC_{(PM2.5)}/TC_{(PM10)}$ ratios for all burns in smoldering (empty squares) and flaming (filled circles) conditions. Error bars represent the standard deviation of the mean.

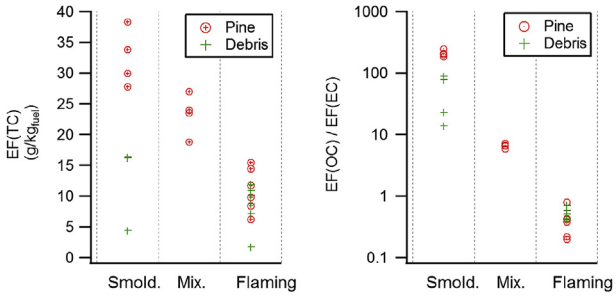

Fig. 3. TC emission factors (left panel) and OC/EC emission ratios (right panel) in PM emitted from smoldering, flaming and mixed phases using pine (red circle) and debris (green cross). (For interpretation of the references to color in this figure legend, the reader is referred to the Web version of this article.)

those conditions, the OC-to-EC ratio ranges from 10 to 100 and from 100 to 300 for debris and pine, respectively. In other words, OC contributes to more than 90% of TC in emissions from both fuels in the smoldering phase. However, a decrease in OC/EC ratios with increasing combustion temperature is observed, which is consistent with previously reported results (Alves et al., 2011; Kocbach Bølling et al., 2009). In mixed phase burns, OC still dominates the emissions, while the OC/EC ratio has decreased by more than an order of magnitude in comparison with the smoldering phase. More precisely, in the mixed phase burns, OC/EC ratios ranged from 5.8 to 7.2 when burning pine. These ratios fall within the range of values reported by Samsonov et al. (2005) in smoke samples from experimental fires in central Siberian Scots pine forests, which supports the fact that the "mixed" mode used in this study simulates reasonably well the conditions that can be found during typical open fire events in the area. In the flaming phase, OC/EC ratios are constantly below 1, indicating that EC dominates the carbon emissions. It is noteworthy to mention that in the smoldering phase the TC as well as the OC fraction is significantly higher when burning pine compared to debris, whereas in flaming burns they are similar for both types of wood.

3.1.3. Organic biomarkers

Emission factors of the compounds identified in smoke from burning pine and debris are given in Table 4. The main organic components found in the smoke particles are saccharide derivatives from the breakdown of cellulose in biomass, phenolic acids from the breakdown of lignin in biomass, accompanied by generally lesser amounts of straight-chain dicarboxylic acids.

Total saccharides are an important group of organics in the smoke emissions, comprising 67% and 11% of the total OC emissions when burning pine and debris, respectively, in the smoldering phase. Much lower contributions of saccharides to the OC emissions (< 0.3%) were found during the burns in flaming phase.

Among saccharides, we distinguish primary sugars, sugar alcohols (polyols) and anhydrosugars (also termed monosaccharide anhydrides) typically derived from wood smoke (Caseiro et al., 2007). As expected, primary sugar concentrations fell below the detections limits, since they are typically at very low abundance in biomass smoke. Sugar alcohols, such as arabitol and mannitol, were found to be emitted only in the smoldering phase of pine and debris, and in much lower quantities than the other measured saccharides.

Emission ratios relative to OC of stereoisomeric anhydrosugars are presented in Fig. 4. For each experiment, levoglucosan (LG) comprises the largest fraction of emitted saccharidic compounds followed by its two isomers, mannosan (MN) and galactosan (GN). The LG-to-OC emission ratio exhibits a great variability depending on the type of biomass burned (see Fig. 5) and combustion conditions. Levoglucosan mass represents about 25% of OC on a mass basis when burning pine in smoldering phase, while it represents only about 5% of OC mass when burning debris in similar temperature conditions. Substantial

Table 4
Emission factors in mg kg_{fuel}^{-1} for saccharides (primary sugars, anhydrosugars, sugar alcohols), dehydroabietic acid, phenolic acids, dicarboxylic acids and related compounds as well as fatty acids in various combinations of fuel and combustion phase.

	Debris smoldering	Debris flaming	Pine smoldering	Pine flaming
• Saccharides:				
Primary sugars (mono and di-saccharides)				
Fructose	< LOD[a]	–[b]	–	< LOD
α-Glucose	< LOD	–	–	< LOD
Sucrose	< LOD	–	–	< LOD
Trehalose	< LOD	–	–	< LOD
Anhydrosugars				
Levoglucosan (LG)	301 ± *187*	12.7 ± *3.59*	7590 ± *336*	4.39
Mannosan (MN)	107 ± *59.6*	< LOD	2430 ± *41.1*	< LOD
Galactosan (GN)	60.1 ± *36.6*	< LOD	405 ± *1.39*	< LOD
LG/MN	2.74 ± *0.17*	–	3.13 ± *0.085*	-
LG/(MN + GN)	1.77 ± *0.08*	–	2.68 ± *0.078*	–
Sugar alcohols				
Arabitol (A)	3.31 ± *0.74*	< LOD	63.4 ± *8.82*	< LOD
Mannitol (M)	3.11 ± *3.20*	< LOD	36.6 ± *4.56*	< LOD
A/M	0.98	–	0.588 ± *0.27*	-
Inositol	0.43	–	–	< LOD
Erythritol	13.8	–	–	< LOD
Glycerol	27	–	–	19.4
EF (Total Saccharides)	**475**	**12.7**	**10520**	**4.39**
• Abietic-type acid (resin acid):				
Dehydroabietic acid	306	20.0	954	0.68
• Phenolic & aromatic acids:				
Syringic acid (O-methylated trihydroxybenzoic acid)	< LOD	< LOD	< LOD	< LOD
Vanillic acid (4-hydroxy 3 methoxybenzoic acid)	4.25	< LOD	245	< LOD
4-Hydroxybenzoic acid	2.67	< LOD	11.2	< LOD
Benzoic acid	62.3	–	–	29.6
• Dicarboxylic acids:				
saturated dicarboxylic acids	66.9	48.92	307	14.7
branched dicarboxylic acids	4.00	0.00	4.59	1.73
unsaturated dicarboxylic acids	73.3	22.22	58.9	15.7
Oxodicarboxylic acids	0.00	5.01	1.04	0.88
EF (dicarboxylic acids)	**144**	**76**	**372**	**33.1**
• Keto-carboxylic acids	2.55	0.00	48.2	0.63
• α-Dicarbonyls	12.1	4.11	48.3	3.85
• Fatty acids	98.7	38.9	12.8	25.6

Standard deviations are given when replicates are available; see Table 1.
[a] LOD is limit of detection.
[b] "-" means there are no available measurements.

differences by more than an order of magnitude in the emission ratios are also observed between flaming and smoldering phases, with higher emission ratios of anhydrosugars in the smoldering phase. Similar variability is observed for its isomers, although the emitted amounts of mannosan and galactosan are substantially lower compared to levoglucosan. This is the reason why levoglucosan is usually preferred as molecular marker of wood smoldering combustion (Engling et al., 2006a; Fraser and Lakshmanan, 2000; Giannoni et al., 2012; Iinuma et al., 2009; Pashynska et al., 2002; Puxbaum et al., 2007).

Because levoglucosan, mannosan, and galactosan are emitted in different relative abundance depending on combinations of burn phase and fuel, the LG/MN (or LG/(MN + GN)) ratio can be used to trace the type of biomass burned. As these compounds are relatively stable in the atmosphere, their emission ratios can also be compared with observed ambient ratios in the atmosphere. From previous chamber experiments (see Fig. 6) it has been found that the LG/MN ratio is in the range of 2.5–6.7 for softwood, while a significantly higher ratio (mean value: 26.7) has been suggested for hardwood (Cheng et al., 2013; Fabbri et al., 2009; Fine et al., 2002, 2004; Schmidl et al., 2008). In our study, a LG/MN ratio of about 3 is observed for smoldering and mixed conditions (for both pine and debris) and of about 2 for flaming which is consistent with the previously reported ratios for softwood (Jung et al.,

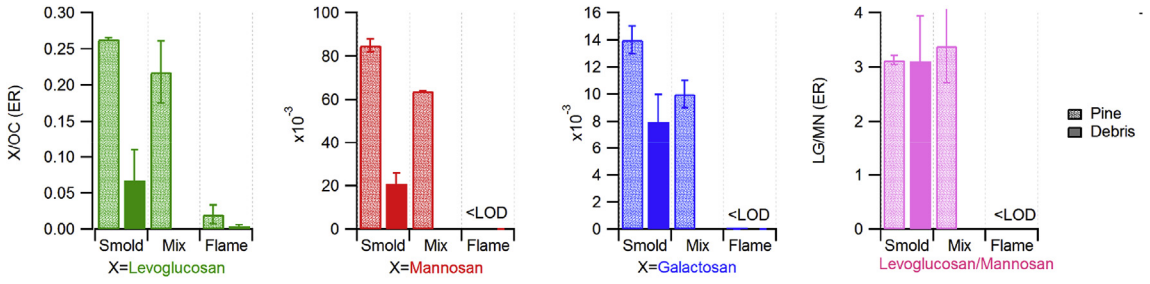

Fig. 4. Emission ratios (ER) of anhydrosugars relative to OC, as well as LG/MN ratios in smoldering (Smold), mixed (Mix), and flaming (Flame) phases.

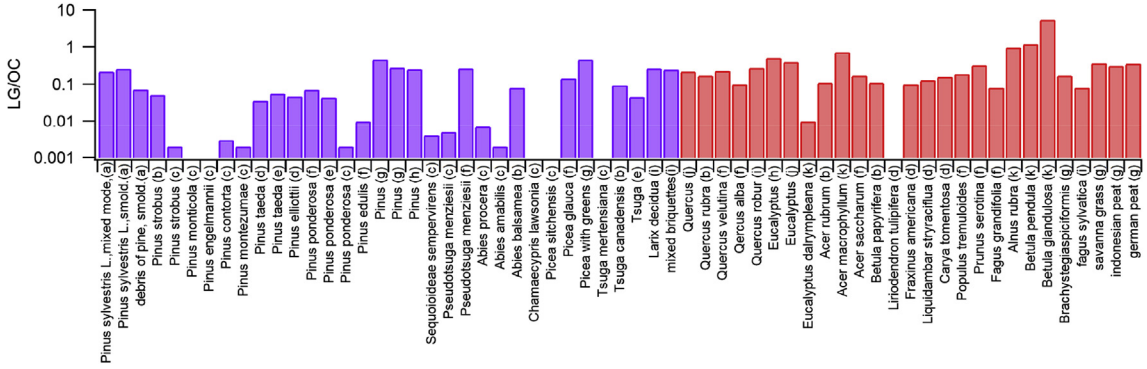

Fig. 5. Comparison of LG/OC emission ratios for different softwood (purple) and hardwood (red) biomass as reported in this study (a) and other references in the literature: (b: Fine et al., 2001), (c: Oros and Simoneit, 2001a), (d: Fine et al., 2002), (e: Hays et al., 2002), (f: Fine et al., 2004), (g: Iinuma et al., 2007), (h: Schauer et al., 2001)), (i: Schmidl et al., 2008), (j: Nolte et al., 2001), (k: Oros and Simoneit, 2001b). (For interpretation of the references to color in this figure legend, the reader is referred to the Web version of this article.)

2016). Similar ratios between 2.7 and 3.5 have been reported in conifer smoke for Apache pine, Douglas fir and Eastern White pines (Oros and Simoneit, 2001b). The ratio determined in our study for smoldering (and mixed) combustion phases is also very similar to the value of 3.4 measured in smoke plumes from Siberian forest fires (Jung et al., 2016).

Dehydroabietic acid is often found to be the second most abundant organic species following levoglucosan. From our study, it appears that dehydroabietic acid is emitted in similar quantities to levoglucosan when burning debris under smoldering conditions, while its emission factor is 3 times lower than that of levoglucosan when burning pine (Table 4). The highest EF of dehydroabietic acid was obtained for pine wood in smoldering conditions.

Among phenolic biomarkers, vanillic (4-hydroxy-3-methoxybenzoic) and 4-hydroxybenzoic acids were detected at levels above the limit of detection only for smoldering burns. Vanillic acid was the most abundant phenolic acid with an EF two orders of magnitude higher in pine smoke compared to debris smoke. This is in agreement with the findings of Simoneit et al. (2000) who reported that the phenol substitution, 3-methoxy-4-hydroxy, pattern is consistent with an origin from gymnosperm (softwood).

A series of saturated dicarboxylic acids (C_2−C_{11}), branched-chain diacids (iC_4-iC_6), unsaturated diacids (M: maleic, F: fumaric and mM: methylmaleic), aromatic diacids (Ph: phthalic, iPh: isophthalic and tPh: terephthalic), hydroxy diacid (hC_4: malic), diacids with a keto-group (kC_3: ketomalonic, and kC_7: 4-ketopimelic), oxocarboxylic acids ($C_{2\omega}$-$C_{9\omega}$, Pyr) and α-dicarbonyls (glyoxal and methylglyoxal) were identified in the smoke samples. The molecular distribution of these compounds resulting from burning pine and debris in each phase is shown in Fig. 7. Emission factors of saturated dicarboxylic diacids, aromatic acids and α-dicarbonyls are significantly higher than those of branched-chain diacids, unsaturated diacids or oxocarboxylic acids for all biofuel/phase combination (Table 4).

Among the saturated n-dicarboxylic acids (C_2−C_{12}), azelaic (C_9) and succinic (C_4) acids are the most abundant followed by glutaric (C_5) and oxalic (C_2) acids. These findings are different from what has been reported in previous studies for ambient continental aerosols where oxalic acid (C_2) was usually found as the most abundant diacid, followed by malonic (C_3) and succinic (C_4) acids (Kawamura et al., 2013; Kundu et al., 2010; Wang et al., 2012). However, high concentrations of azelaic acid in Siberian BB plumes have been already reported in the past (Agarwal et al., 2010). As a matter of fact, azelaic acid has been identified as a specific oxidation product of unsaturated fatty acids contained in biomass smoke (Kawamura et al., 2013).

It is worth mentioning here that C_3/C_4 ratios in the pine/smoldering burn are always below 0.03, whereas in the remaining burns (pine/flame, debris/flame and debris/smoldering), C_3 levels are below the method detection limit, thus resulting ratios would have been even lower. These values are significantly lower than those in vehicle exhaust (0.22–0.44), ambient urban aerosols which have experienced photochemical aging (0.4–1.0), and photochemically aged marine aerosols (> 2.0) (Kawamura and Bikkina, 2016).

3.2. Evolution of biomass burning aerosols

Following emission and dispersion in the chamber, BB aerosols undergo various physical and chemical transformations, including coagulation, interaction with gaseous species, and deposition. Distinguishing between fresh and aged organic aerosols gives an

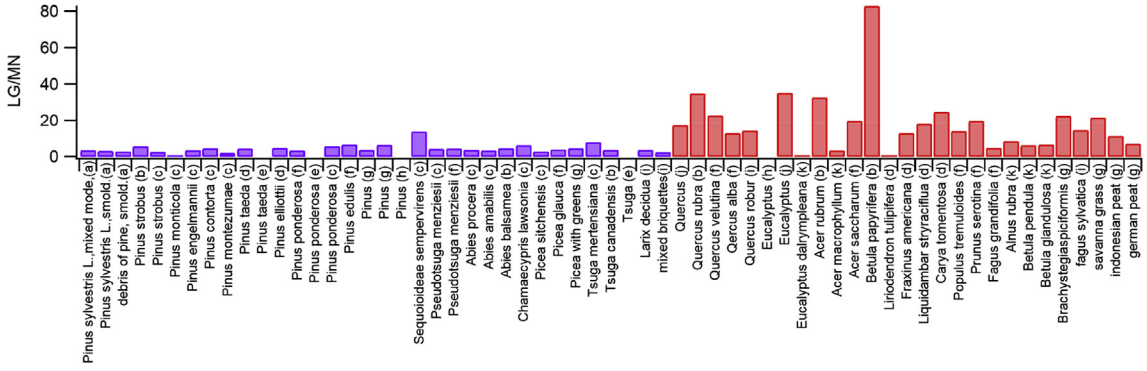

Fig. 6. Comparison of LG/MN ratios for different softwood (purple) and hardwood (red) biomass as reported in this study (a) and other references in the literature: (b: Fine et al., 2001), (c: Oros and Simoneit, 2001a), (d: Fine et al., 2002), (e: Hays et al., 2002), (f: Fine et al., 2004), (g: Iinuma et al., 2007), (h: Schauer et al., 2001)), (i: Schmidl et al., 2008), (j: Nolte et al., 2001), (k: Oros and Simoneit, 2001b). (For interpretation of the references to color in this figure legend, the reader is referred to the Web version of this article.)

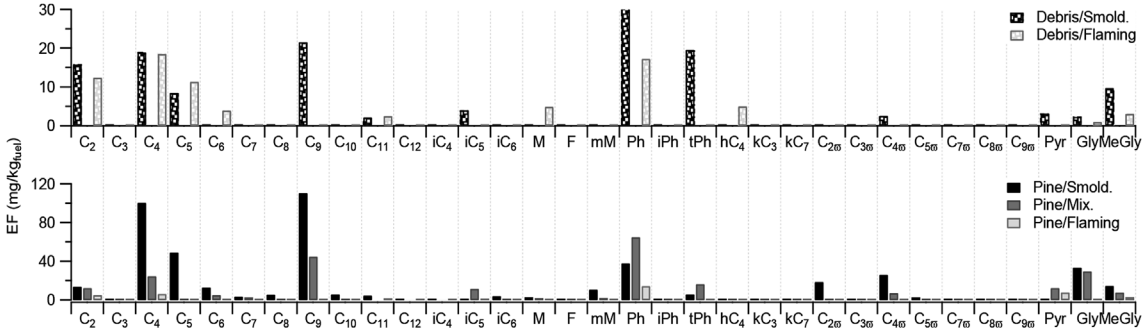
Debris/Smold.
Debris/Flaming
Pine/Smold.
Pine/Mix.
Pine/Flaming
EF (mg/kg$_{fuel}$)
C$_2$ C$_3$ C$_4$ C$_5$ C$_6$ C$_7$ C$_8$ C$_9$ C$_{10}$ C$_{11}$ C$_{12}$ iC$_4$ iC$_5$ iC$_6$ M F mM Ph iPh tPh hC$_4$ kC$_3$ kC$_7$ C$_{2ω}$ C$_{3ω}$ C$_{4ω}$ C$_{5ω}$ C$_{7ω}$ C$_{8ω}$ C$_{9ω}$ Pyr GlyMeGly

Fig. 7. Molecular distributions of dicarboxylic acids and related compounds.

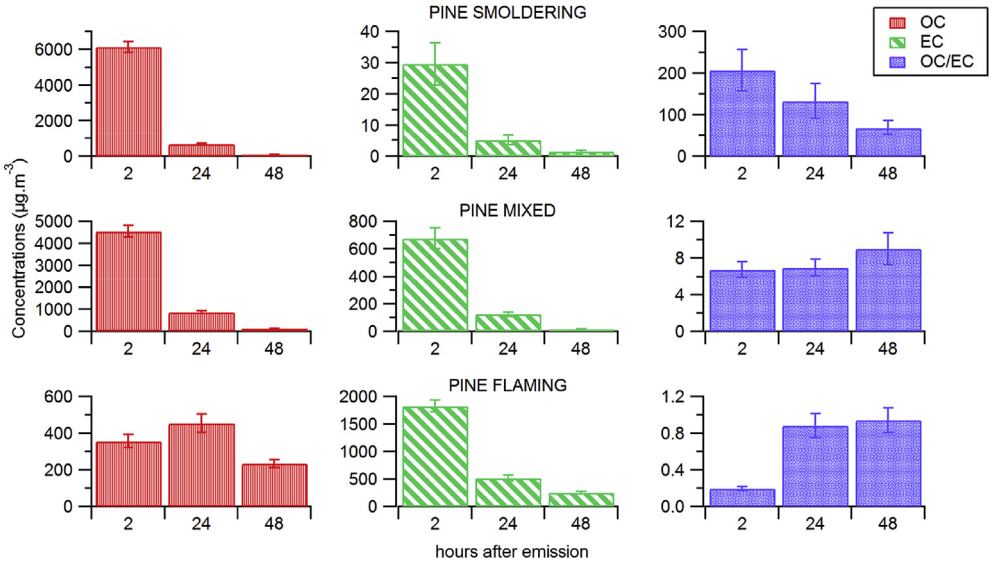

Fig. 8. Time evolution of concentrations of OC (red), EC (green) and OC/EC ratios (blue) during dark aging. (For interpretation of the references to color in this figure legend, the reader is referred to the Web version of this article.)

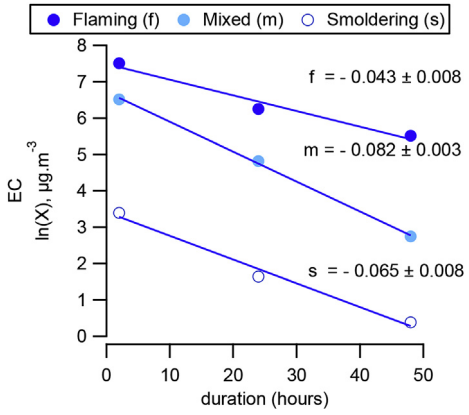

Fig. 9. Concentration of EC versus time. The slope of regression represents the loss rate. Values of slopes are denoted *s, m, and f* for smoldering, mixed and flaming phases of pine burning, respectively.

indication of how processing influences the atmospheric loading and composition of organic aerosols.

Elemental carbon is used here as a reference for evaluating losses due to aerosol dynamics (diffusion, convective deposition and gravitational settling), because it is produced only as primary product of incomplete combustion and is a chemically inert specie. The aim of this study was not only to chemically identify a large number of species but to further elucidate whether any of those species underwent chemical transformations under dark conditions. The method of comparison to inert species like EC allows the quantitative detection of such processes in terms of loss or generation of the organic compounds described above.

Fig. 8 illustrates the time evolution of OC, EC and OC/EC ratios for pine burning in smoldering, mixed and flaming phases. As expected, OC and EC concentrations decrease with time due to deposition and wall losses in the chamber. However, OC and EC do not decrease with the same rate, and therefore OC/EC ratios evolve with aging. OC/EC variation demonstrates a changing rate of OC enhancement through secondary formation and OC loss through physical processes and chemical transformations during aging.

For instance, Fenton reactions could possibly occur in the dark chamber, i.e., Fe(II) and H_2O_2 can react in aqueous particles to produce OH radicals which can oxidize organic species to result in carboxylic acids or other oxidation products, although such reactions are inherently dependent on the presence of water and iron in the smoke aerosol (Zepp et al., 1992). Additional transformation processes such as oligomerization of semi-volatile organic species (SVOCs) could also occur on particles in dark conditions, e.g., as a result of ester or hemiacetal formation (Tolocka et al., 2004).

In the smoldering phase, OC/EC ratios decrease by a factor of almost 4 between fresh samples and 48-h aged samples. In terms of relative contribution, OC represents about 96% of total $PM_{2.5}$ mass in fresh versus 85% in 48-h aged aerosol (Fig. 6). The fact that OC decreases faster than EC suggests a sink of OC such as evaporation of semi-volatile organic compounds or chemical degradation of reactive organic species

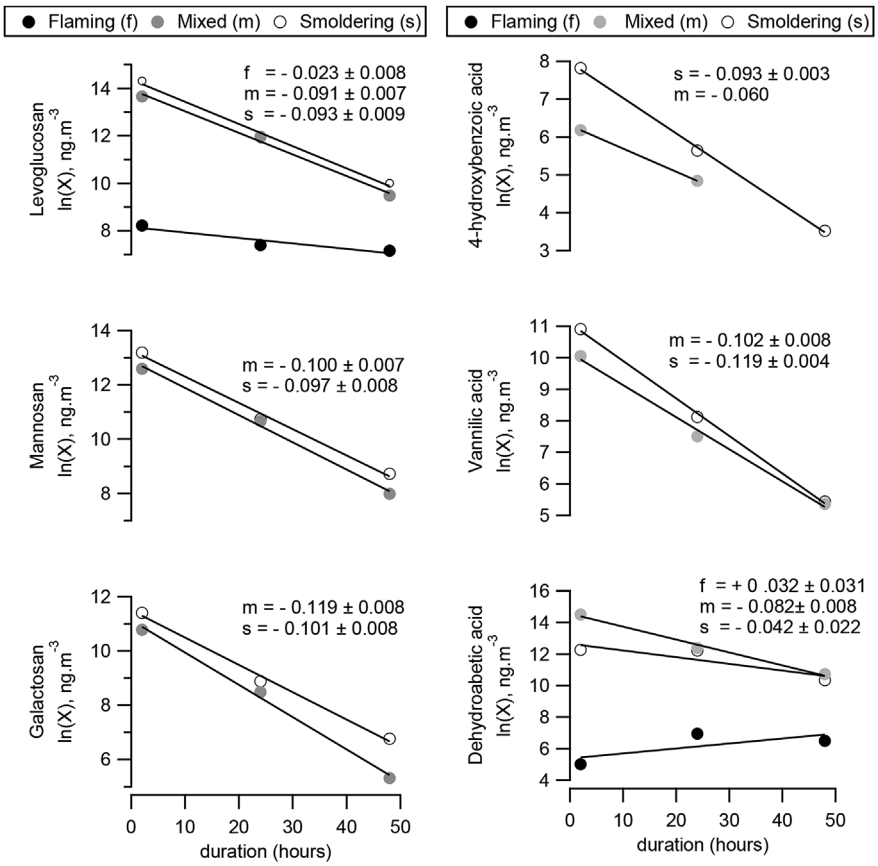
Flaming (f)
Mixed (m)
Smoldering (s)
Levoglucosan ln(X), ng.m-3
f = - 0.023 ± 0.008
m = - 0.091 ± 0.007
s = - 0.093 ± 0.009
4-hydroxybenzoic acid ln(X), ng.m-3
s = - 0.093 ± 0.003
m = - 0.060
Mannosan ln(X), ng.m-3
m = - 0.100 ± 0.007
s = - 0.097 ± 0.008
Vanillic acid ln(X), ng.m-3
m = - 0.102 ± 0.008
s = - 0.119 ± 0.004
Galactosan ln(X), ng.m-3
m = - 0.119 ± 0.008
s = - 0.101 ± 0.008
Dehydroabetic acid ln(X), ng.m-3
f = + 0 .032 ± 0.031
m = - 0.082± 0.008
s = - 0.042 ± 0.022
duration (hours)
duration (hours)

Fig. 10. Concentrations of selected anhydrosugars (LG, MN, GN), phenolic acids (4-OH benzoic and vanillic acids), as well as resin acids (dehydroabietic acid) versus time. The slope of regression represents loss rates. The values of slopes are denoted s, m, and f for smoldering, mixed and flaming phases of pine burning, respectively.

(in the OC-dominant smoke particles), reducing OC concentrations to a greater degree than would be expected from deposition or wall losses alone. It also suggests that there is no significant secondary production of OC, since organics are already condensed at the time of the smoke emission or shortly after (during cooling and dilution) and/or the freshly produced organic-rich smoke aerosol inhibits further aerosol production for smoldering fires.

In contrast, in the flaming phase, the OC/EC ratios increase from about 0.2 to about 1, suggesting that there is production and condensation of organics after the fresh smoke emission. In terms of relative contribution, OC represents about 21% of $PM_{2.5}$ mass for fresh versus 46% for 48-h aged aerosols (Fig. 8), whereas the relative contribution of elemental carbon decreases from 54% to 25%. This significant OC enhancement possibly occurs due to production of reactive precursors under the high temperatures present during flaming combustion (Gao et al., 2003), followed by gas-to-particle conversion in form of condensation of semi-volatile organic species onto soot particles during the first 24 h of smoke aging. Condensation of organics from flaming burns seems to occur much later following emission compared to smoldering fires, warranting further investigation. The oligomerization of semi-volatile species, e.g., in form of ester or hemiacetal formation, is known to be a slow process which would occur on time scales of days, and could thus explain our observations to some extent. In a recent study of biomass smoke evolution, aging in the dark (over a short time period of a few hours) also resulted in increased organic aerosol loadings (up to a factor of two) and specifically formation of secondary organic nitrogen compounds due to the oxidation of VOCs by NO_3 radicals, although no distinction of combustion phase (smoldering vs flaming) was made in that study (Tiitta et al., 2016).

An intermediate evolution is observed for mixed fires, with OC/EC ratios increasing from day to day although at a very low rate of change. Overall, it is obvious and has been pointed out for other studies (e.g., Heringa et al., 2011) that a complex combination of processes takes place during biomass smoke aging, including condensation and evaporation, as well as oxidation resulting in fragmentation or further functionalization.

In order to investigate the response of biomass markers to physical and chemical processing, the experimentally determined loss rate coefficients of components of BB aerosol are compared to the EC loss rate coefficient. Following the release of smoke into the air-tight LAC chamber, the particle concentration C_t decay with time can be expressed as

$$C_t = C_{t=0} \times e^{-\beta \times t} \quad (4)$$

where t is the elapsed time, $C_{t=0}$ is the concentration of fresh aerosols and β is the particle decay rate loss coefficient. In this expression, β incorporates the processes that remove particles in the enclosure (e.g., diffusion loss, gravitational settling, and other loss mechanisms by external forces) (Lai, 2002). The EC decay loss rate coefficient is derived by plotting ln*(EC)* versus time and calculating the slope of the fitted line.

As illustrated in Fig. 9, the EC loss rate varies between 0.043 ± 0.008 and 0.082 ± 0.003 h^{-1}. Based on this finding, we assume that the loss rate of particles due to diffusion and gravitational settling inside the chamber is about 0.060 ± 0.025 h^{-1}. The determined particle loss rate coefficient does not take into account the coagulation and other processes such as evaporation and condensation, assuming EC as chemically stable species. We therefore calculate the loss rate of other compounds, and assume that higher values of loss rates are evidence of additional sinks, whereas lower values suggest potential secondary formation.

The loss rates of selected individual phenolic acids, saccharidic

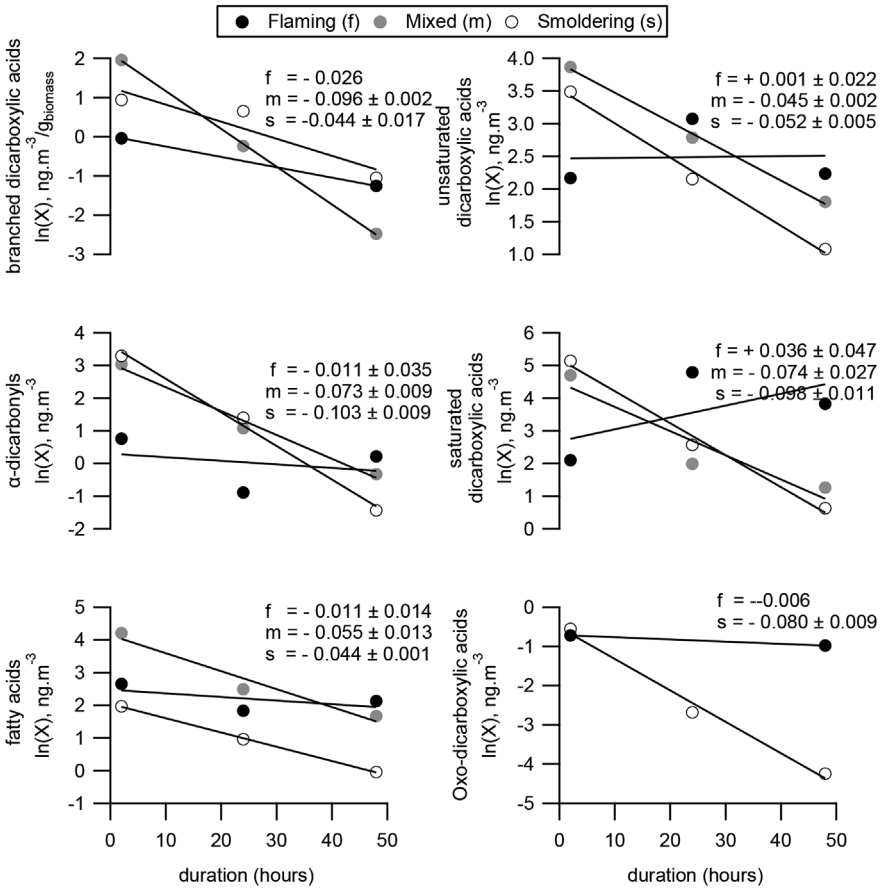
Flaming (f)
Mixed (m)
Smoldering (s)
branched dicarboxylic acids ln(X), ng.m-3/gbiomass
f = - 0.026
m = - 0.096 ± 0.002
s = -0.044 ± 0.017
unsaturated dicarboxylic acids ln(X), ng.m-3
f = + 0.001 ± 0.022
m = - 0.045 ± 0.002
s = - 0.052 ± 0.005
α-dicarbonyls ln(X), ng.m-3
f = - 0.011 ± 0.035
m = - 0.073 ± 0.009
s = - 0.103 ± 0.009
saturated dicarboxylic acids ln(X), ng.m-3
f = + 0.036 ± 0.047
m = - 0.074 ± 0.027
s = - 0.098 ± 0.011
fatty acids ln(X), ng.m-3
f = - 0.011 ± 0.014
m = - 0.055 ± 0.013
s = - 0.044 ± 0.001
Oxo-dicarboxylic acids ln(X), ng.m-3
f = --0.006
s = - 0.080 ± 0.009
duration (hours)
duration (hours)

Fig. 11. Concentrations of the sum of carboxylic acids (grouped in families depending on their functional group) versus time after emission. The slope of the regression represents the calculated loss rates for specific compounds in the chamber. The values of the slopes are denoted s, m or f for smoldering, mixed and flaming burning of pine, respectively. Keto-carboxylic acids are not shown here due to limited number of data points.

compounds and resin acids are presented in Fig. 10. In Fig. 11, the loss rates of the sum of compounds belonging to selected carboxylic acid families are shown.

In the flaming phase, many species exhibit a negative slope, but with a lower loss rate than that of EC. This is the case for levoglucosan, the sum of fatty acids, sum of oxo-dicarboxylic acids, α-dicarbonyls and branched dicarboxylic acids, thereby indicating a degradation and/or wall loss and deposition after the initial emission from flaming burns. Other compounds such as dehydroabietic acid as well as the sum of saturated and unsaturated dicarboxylic acids exhibit a positive slope for the flaming phase, suggesting SOA formation exceeding other losses.

In the smoldering phase, for all smoke constituents studied, the slope(s) representing the loss rate is always within the range, or slightly higher, to the values attributed to EC which is assumed to correspond to deposition and wall losses. This finding supports the conclusion that no significant chemical transformation occurs for smoke particle composition in the smoldering phase. The slightly higher values indicate an additional sink such as possible evaporation of semi-volatile compounds or degradation of certain species due to their higher reactivity.

4. Conclusions

This work presents a detailed chemical characterization of biomass burning aerosols emitted from the combustion of Siberian wood species. Small-scale fires were conducted in a combustion chamber and were designed to distinguish and study separately the emissions from the different combustion phases (smoldering vs flaming). Coarse and fine smoke aerosols were sampled and analyzed for a large variety of carboxylic acids and sugars, as well as OC and EC.

Aerosol mass was strongly dominated by particles in the sub-2.5 μm diameter size range, and no significant difference was observed in the carbon fraction composition between fine and coarse aerosols. Higher emission factors of particle mass were observed when burning pine compared to debris. For pine, EF(PM_X) in the smoldering phase were on average 5 times higher than in flaming burns. Significantly higher loadings of organic species were found in our smoldering BB aerosols than in the aerosols emitted in the flaming phase. Under low-temperature combustion condition, OC contributed to more than 90% of TC in emissions from both fuels, whereas in the flaming phase EC dominated the emissions. Based on these results, we conclude that emission factors for OC and $PM_{2.5}$ are strong functions of combustion conditions. Emission factors of organics are also strongly dependent on the type of plant species burned under smoldering conditions but weekly depend on the plant species for flaming conditions.

Anhydrosugars were the most abundant compound group in the aerosol particles derived from the combustion of both biofuel types. The ratios of levoglucosan/mannosan were about 3 for smoldering and mixed conditions (for both pine and debris) and about 2 for flaming burns, which is consistent with previously reported values for softwood. Dehydroabietic acid was emitted in similar quantities to levoglucosan during the burning of debris under smoldering conditions, while its emission factor was lower compared to that of levoglucosan during the burning of pine. Among phenolic biomarkers, vanillic and 4-hydroxybenzoic acids were detected at levels above the limit of detections only for smoldering burns. Other individual compounds, such as azelaic and succinic acids, have been found in significant quantities as well. From the molecular distributions of dicarboxylic acids and related compounds, it appears that the molecular composition of fresh biomass burning aerosols is very different from those in motor vehicle exhaust and ambient aerosols.

The ratios of selected biomarkers over total OC can be a useful tool for distinguishing the type of wood burned and contribution of combustion phases in natural fires.

Indications of SOA production under dark conditions after flaming

fires were suggested by the results of this study. On the other hand, no evidence of chemical transformation was obtained for smoke particles emitted in the smoldering phase.

Further combustion studies are needed for the investigation of subsequent aging processes specifically for Siberian fire emissions, including oxidation in the presence of sunlight, in order to obtain a more comprehensive understanding of the environmental impact and to make more accurate predictions on climate forcing of such biomass burning emissions. Specifically, better understanding of the chemical and physical characteristics of organic smoke components is needed, as they may have significant influence on climate forcing via the indirect aerosol effect, depending on the polarity and thus hygroscopicity of the individual organic species, which is determined by the combustion phase and degree of aging.

Acknowledgments

This work was supported by (1) EnTeC FP7 Capacities program (REGPOT-2012-2013-1, FP7, ID: 316173) and 2) RFBR 12-05-90802, 12-05-00395 projects and (3) NSC-RFBR 12-05-92002 project.

References

Agarwal, S., Aggarwal, S.G., Okuzawa, K., Kawamura, K., 2010. Size distributions of dicarboxylic acids, ketoacids, α-dicarbonyls, sugars, WSOC, OC, EC and inorganic ions in atmospheric particles over Northern Japan: implication for long-range transport of Siberian biomass burning and East Asian polluted aerosols. Atmos. Chem. Phys. 10 (13), 5839–5858. http://dx.doi.org/10.5194/acp-10-5839-2010.

Alves, C., Gonçalves, C., Fernandes, A.P., Tarelho, L., Pio, C., 2011. Fireplace and woodstove fine particle emissions from combustion of western Mediterranean wood types. Atmos. Res. 101 (3), 692–700. http://dx.doi.org/10.1016/j.atmosres.2011.04.015.

Alves, C.A., Gonçalves, C., Pio, C.A., Mirante, F., Caseiro, A., Tarelho, L., Freitas, M.C., Viegas, D.X., 2010. Smoke emissions from biomass burning in a Mediterranean shrubland. Atmos. Environ. 44 (25), 3024–3033. http://dx.doi.org/10.1016/j.atmosenv.2010.05.010.

Alves, C.A., Vicente, E.D., Rocha, S., Vicente, A.M., 2016. Organic tracers in aerosols from the residential combustion of pellets and agro-fuels. Air Qual. Atmosphere Health 1–9. http://dx.doi.org/10.1007/s11869-016-0406-3.

AMAP, 2012. Arctic climate issues 2011: changes in arctic snow, water, ice and permafrost | AMAP. [online] Available from. http://www.amap.no/documents/doc/arctic-climate-issues-2011-changes-in-arctic-snow-water-ice-and-permafrost/129, Accessed date: 18 November 2016.

Amiridis, V., Zerefos, C., Kazadzis, S., Gerasopoulos, E., Eleftheratos, K., Vrekoussis, M., Stohl, A., Mamouri, R.E., Kokkalis, P., Papayannis, A., 2012. Impact of the 2009 Attica wild fires on the air quality in urban Athens. Atmos. Environ. 46, 536–544.

Bond, T.C., Doherty, S.J., Fahey, D.W., Forster, P.M., Berntsen, T., DeAngelo, B.J., Flanner, M.G., Ghan, S., Kärcher, B., Koch, D., Kinne, S., Kondo, Y., Quinn, P.K., Sarofim, M.C., Schultz, M.G., Schulz, M., Venkataraman, C., Zhang, H., Zhang, S., Bellouin, N., Guttikunda, S.K., Hopke, P.K., Jacobson, M.Z., Kaiser, J.W., Klimont, Z., Lohmann, U., Schwarz, J.P., Shindell, D., Storelvmo, T., Warren, S.G., Zender, C.S., 2013. Bounding the role of black carbon in the climate system: a scientific assessment. J. Geophys. Res. Atmospheres 118 (11), 5380–5552. http://dx.doi.org/10.1002/jgrd.50171.

Boucher, O., Randall, D., Artaxo, P., Bretherton, C., Feingold, G., Forster, P., Kerminen, V.-M., Kondo, Y., Liao, H., Lohmann, U., Rasch, P., Satheesh, S.K., Sherwood, S., Stevens, B., Zhang, X.Y., 2013. Clouds and aerosols. In: Stocker, T.F., Qin, D., Plattner, G.-K., Tignor, M., Allen, S.K., Boschung, J., Nauels, A., Xia, Y., Bex, V., Midgley, P.M. (Eds.), Climate Change 2013: The Physical Science Basis. Contribution of Working Group I to the Fifth Assessment Report of the Intergovernmental Panel on Climate Change. Cambridge University Press, Cambridge, United Kingdom and New York, NY, USA, pp. 571–658. https://doi.org/10.1017/CBO9781107415324.016.

Carrico, C.M., Petters, M.D., Kreidenweis, S.M., Sullivan, A.P., McMeeking, G.R., Levin, E.J.T., Engling, G., Malm, W.C., Collett Jr., J.L., 2010. Water uptake and chemical composition of fresh aerosols generated in open burning of biomass. Atmos. Chem. Phys. 10, 5165–5178. https://doi.org/10.5194/acp-10-5165-2010.

Caseiro, A., Marr, I.L., Claeys, M., Kasper-Giebl, A., Puxbaum, H., Pio, C.A., 2007. Determination of saccharides in atmospheric aerosol using anion-exchange high-performance liquid chromatography and pulsed-amperometric detection. J. Chromatogr. A 1171 (1), 37–45. http://dx.doi.org/10.1016/j.chroma.2007.09.038.

Cavalli, F., Viana, M., Yttri, K.E., Genberg, J., Putaud, J.-P., 2010. Toward a standardised thermal-optical protocol for measuring atmospheric organic and elemental carbon: the EUSAAR protocol. Atmos Meas Tech 3 (1), 79–89. http://dx.doi.org/10.5194/amt-3-79-2010.

Cheng, Y., Engling, G., He, K.-B., Duan, F.-K., Ma, Y.-L., Du, Z.-Y., Liu, J.-M., Zheng, M., Weber, R.J., 2013. Biomass burning contribution to Beijing aerosol. Atmos. Chem. Phys. 13 (15), 7765–7781. http://dx.doi.org/10.5194/acp-13-7765-2013.

Chow, J.C., Watson, J.G., Chen, L.-W.A., Chang, M.C.O., Robinson, N.F., Trimble, D., Kohl, S., 2007. The IMPROVE_A temperature protocol for thermal/optical carbon analysis: maintaining consistency with a long-term database. J. Air Waste Manag. Assoc. 57 (9), 1014–1023. http://dx.doi.org/10.3155/1047-3289.57.9.1014.

Cocker, D.R., Flagan, R.C., Seinfeld, J.H., 2001. State-of-the-Art chamber facility for studying atmospheric aerosol chemistry. Environ. Sci. Technol. 35 (12), 2594–2601. http://dx.doi.org/10.1021/es0019169.

Damoah, R., Spichtinger, N., Forster, C., James, P., Mattis, I., Wandinger, U., Beirle, S., Wagner, T., Stohl, A., 2004. Around the world in 17 days - hemispheric-scale transport of forest fire smoke from Russia in May 2003. Atmospheric Chem. Phys. 4, 1311–1321. https://doi.org/10.5194/acp-4-1311-2004.

Deshmukh, D.K., Kawamura, K., Lazaar, M., Kunwar, B., Boreddy, S.K.R., 2016. Dicarboxylic acids, oxoacids, benzoic acid, α-dicarbonyls, WSOC, OC, and ions in spring aerosols from Okinawa Island in the western North Pacific Rim: size distributions and formation processes. Atmos. Chem. Phys. 16 (8), 5263–5282. http://dx.doi.org/10.5194/acp-16-5263-2016.

Diapouli, E., Popovicheva, O., Kistler, M., Vratolis, S., Persiantseva, N., Timofeev, M., Kasper-Giebl, A., Eleftheriadis, K., 2014. Physicochemical characterization of aged biomass burning aerosol after long-range transport to Greece from large scale wildfires in Russia and surrounding regions, Summer 2010. Atmos. Environ. 96 (Suppl. C), 393–404. http://dx.doi.org/10.1016/j.atmosenv.2014.07.055.

Donahue, N.M., Robinson, A.L., Stanier, C.O., Pandis, S.N., 2006. Coupled partitioning, dilution, and chemical aging of semivolatile organics. Environ. Sci. Technol. 40 (8), 2635–2643.

Engling, G., Herckes, P., Kreidenweis, S.M., Malm, W.C., Collett Jr., J., 2006a. L.: Composition of the fine organic aerosol in Yosemite National Park during the 2002 Yosemite Aerosol Characterization Study. Atmos. Environ. 40 (16), 2959–2972. http://dx.doi.org/10.1016/j.atmosenv.2005.12.041.

Engling, G., Carrico, C.M., Kreidenweis, S.M., Collett Jr., J.L., Day, D.E., Malm, W.C., Lincoln, E., Hao, W.M., Iinuma, Y., Herrmann, H., 2006b. Determination of levoglucosan in biomass combustion aerosol by high-performance anion-exchange chromatography with pulsed amperometric detection. Atmos. Environ. 40 (Suppl. 2), 299–311. https://doi.org/10.1016/j.atmosenv.2005.12.069.

Fabbri, D., Torri, C., Simoneit, B.R.T., Marynowski, L., Rushdi, A.I., Fabiańska, M.J., 2009. Levoglucosan and other cellulose and lignin markers in emissions from burning of Miocene lignites. Atmos. Environ. 43 (14), 2286–2295. http://dx.doi.org/10.1016/j.atmosenv.2009.01.030.

Fine, P.M., Cass, G.R., Simoneit, B.R., 2001. Chemical characterization of fine particle emissions from fireplace combustion of woods grown in the northeastern United States. Environ. Sci. Technol. 35 (13), 2665–2675.

Fine, P.M., Cass, G.R., Simoneit, B.R.T., 2002. Chemical characterization of fine particle emissions from the fireplace combustion of woods grown in the southern United States. Environ. Sci. Technol. 36 (7), 1442–1451. http://dx.doi.org/10.1021/es0108988.

Fine, P.M., Cass, G.R., Simoneit, B.R.T., 2004. Chemical characterization of fine particle emissions from the fireplace combustion of wood types grown in the midwestern and western United States. Environ. Eng. Sci. 21 (3), 387–409. http://dx.doi.org/10.1089/109287504323067021.

Fraser, M.P., Lakshmanan, K., 2000. Using levoglucosan as a molecular marker for the long-range transport of biomass combustion aerosols. Environ. Sci. Technol. 34 (21), 4560–4564. http://dx.doi.org/10.1021/es991229l.

Fu, P., Kawamura, K., Okuzawa, K., Aggarwal, S.G., Wang, G., Kanaya, Y., Wang, Z., 2008. Organic molecular compositions and temporal variations of summertime mountain aerosols over Mt. Tai, North China Plain. J. Geophys. Res. Atmospheres 113 (D19) [online] Available from. http://onlinelibrary.wiley.com/doi/10.1029/2008JD009900/full.

Gao, S., Hegg, D.A., Hobbs, P.V., Kirchstetter, T.W., Magi, B.I., Sadilek, M., 2003. Water-soluble organic components in aerosols associated with savanna fires in southern Africa: identification, evolution, and distribution. J. Geophys. Res. Atmospheres 108 (D13) [online] Available from. http://onlinelibrary.wiley.com/doi/10.1029/2002JD002324/full.

Giannoni, M., Martellini, T., Bubba, M.D., Gambaro, A., Zangrando, R., Chiari, M., Lepri, L., Cincinelli, A., 2012. The use of levoglucosan for tracing biomass burning in PM2.5 samples in Tuscany (Italy). Environ. Pollut. 167 (Suppl. C), 7–15. https://doi.org/10.1016/j.envpol.2012.03.016.

Grieshop, A.P., Logue, J.M., Donahue, N.M., Robinson, A.L., 2009. Laboratory investigation of photochemical oxidation of organic aerosol from wood fires 1: measurement and simulation of organic aerosol evolution. Atmos. Chem. Phys. 9 (4), 1263–1277. http://dx.doi.org/10.5194/acp-9-1263-2009.

Hays, M.D., Geron, C.D., Linna, K.J., Smith, N.D., Schauer, J.J., 2002. Speciation of gas-phase and fine particle emissions from burning of foliar fuels. Environ. Sci. Technol. 36 (11), 2281–2295. http://dx.doi.org/10.1021/es0111683.

Hennigan, C.J., Sullivan, A.P., Collett, J.L., Robinson, A.L., 2010. Levoglucosan stability in biomass burning particles exposed to hydroxyl radicals. Geophys. Res. Lett. 37 (9), L09806. http://dx.doi.org/10.1029/2010GL043088.

Hennigan, C.J., Miracolo, M.A., Engelhart, G.J., May, A.A., Presto, A.A., Lee, T., Sullivan, A.P., McMeeking, G.R., Coe, H., Wold, C.E., Hao, W.-M., Gilman, J.B., Kuster, W.C., de Gouw, J., Schichtel, B.A., Collett Jr., J.L., Kreidenweis, S.M., Robinson, A.L., 2011. Chemical and physical transformations of organic aerosol from the photo-oxidation of open biomass burning emissions in an environmental chamber. Atmos. Chem. Phys. 11 (15), 7669–7686. http://dx.doi.org/10.5194/acp-11-7669-2011.

Heringa, M.F., DeCarlo, P.F., Chirico, R., Tritscher, T., Dommen, J., Weingartner, E., Richter, R., Wehrle, G., Prévôt, A.S.H., Baltensperger, U., 2011. Investigations of primary and secondary particulate matter of different wood combustion appliances with a high-resolution time-of-flight aerosol mass spectrometer. Atmos. Chem. Phys. 11 (12), 5945–5957. http://dx.doi.org/10.5194/acp-11-5945-2011.

Hoffmann, D., Tilgner, A., Iinuma, Y., Herrmann, H., 2010. Atmospheric stability of levoglucosan: a detailed laboratory and modeling study. Environ. Sci. Technol. 44 (2),

694–699. http://dx.doi.org/10.1021/es902476f.
Hosseini, S., Li, Q., Cocker, D., Weise, D., Miller, A., Shrivastava, M., Miller, J.W., Mahalingam, S., Princevac, M., Jung, H., 2010. Particle size distributions from laboratory-scale biomass fires using fast response instruments. Atmos. Chem. Phys. 10, 8065–8076.
Iinuma, Y., Brüggemann, E., Gnauk, T., Müller, K., Andreae, M.O., Helas, G., Parmar, R., Herrmann, H., 2007. Source characterization of biomass burning particles: the combustion of selected European conifers, African hardwood, savanna grass, and German and Indonesian peat. J. Geophys. Res. Atmospheres 112 (D8), D08209. http://dx.doi.org/10.1029/2006JD007120.
Iinuma, Y., Engling, G., Puxbaum, H., Herrmann, H., 2009. A highly resolved anion-exchange chromatographic method for determination of saccharidic tracers for biomass combustion and primary bio-particles in atmospheric aerosol. Atmos. Environ. 43 (6), 1367–1371. http://dx.doi.org/10.1016/j.atmosenv.2008.11.020.
Jung, J., Lyu, Y., Lee, M., Hwang, T., Lee, S., Oh, S., 2016. Impact of Siberian forest fires on the atmosphere over the Korean Peninsula during summer 2014. Atmos. Chem. Phys. 16 (11), 6757–6770. http://dx.doi.org/10.5194/acp-16-6757-2016.
Kasischke, E.S., Penner, J.E., 2004. Improving global estimates of atmospheric emissions from biomass burning. J. Geophys. Res. Atmospheres 109 (D14) [online] Available from. http://onlinelibrary.wiley.com/doi/10.1029/2004JD004972/full, Accessed date: 18 November 2016.
Kavouras, I.G., Nikolich, G., Etyemezian, V., Dubois, D.W., King, J., Shafer, D., 2012. In situ observations of soil minerals and organic matter in the early phases of prescribed fires. J. Geophys. Res. Atmospheres 117 (12). http://dx.doi.org/10.1029/2011JD017420.
Kawamura, K., 1993. Identification of C2-C10.omega.-oxocarboxylic acids, pyruvic acid, and C2-C3.alpha.-dicarbonyls in wet precipitation and aerosol samples by capillary GC and GC/MS. Anal. Chem. 65 (23), 3505–3511. http://dx.doi.org/10.1021/ac00071a030.
Kawamura, K., Bikkina, S., 2016. A review of dicarboxylic acids and related compounds in atmospheric aerosols: molecular distributions, sources and transformation. Atmos. Res. 170 (Suppl. C), 140–160. http://dx.doi.org/10.1016/j.atmosres.2015.11.018.
Kawamura, K., Ikushima, K., 1993. Seasonal changes in the distribution of dicarboxylic acids in the urban atmosphere. Environ. Sci. Technol. 27 (10), 2227–2235. http://dx.doi.org/10.1021/es00047a033.
Kawamura, K., Tachibana, E., Okuzawa, K., Aggarwal, S.G., Kanaya, Y., Wang, Z.F., 2013. High abundances of water-soluble dicarboxylic acids, ketocarboxylic acids and α-dicarbonyls in the mountaintop aerosols over the North China Plain during wheat burning season. Atmos. Chem. Phys. 13 (16), 8285–8302. http://dx.doi.org/10.5194/acp-13-8285-2013.
Kirchgeorg, T., Schüpbach, S., Kehrwald, N., McWethy, D.B., Barbante, C., 2014. Method for the determination of specific molecular markers of biomass burning in lake sediments. Org. Geochem. 71, 1–6. http://dx.doi.org/10.1016/j.orggeochem.2014.02.014.
Kleeman, M.J., Schauer, J.J., Cass, G.R., 1999. Size and composition distribution of fine particulate matter emitted from wood burning, meat charbroiling, and cigarettes. Environ. Sci. Technol. 33 (20), 3516–3523. http://dx.doi.org/10.1021/es981277q.
Koch, D., Menon, S., Genio, A.D., Ruedy, R., Alienov, I., Schmidt, G.A., 2009. Distinguishing aerosol impacts on climate over the past century. J. Clim 22, 2659–2677. https://doi.org/10.1175/2008JCLI2573.1.
Kocbach Bølling, A., Pagels, J., Yttri, K.E., Barregard, L., Sallsten, G., Schwarze, P.E., Boman, C., 2009. Health effects of residential wood smoke particles: the importance of combustion conditions and physicochemical particle properties. Part. Fibre Toxicol. 6, 29,. http://dx.doi.org/10.1186/1743-8977-6-29.
Kozlov, V.S., Panchenko, M.V., Yausheva, E.P., 2008. Mass fraction of black carbon in submicron aerosol as an indicator of influence of smoke from remote forest fires in Siberia. Atmos. Environ. 42 (11), 2611–2620. http://dx.doi.org/10.1016/j.atmosenv.2007.07.036.
Kozlov, V.S., Yausheva, E.P., Terpugova, S.A., Panchenko, M.V., Chernov, D.G., Shmargunov, V.P., 2014. Optical–microphysical properties of smoke haze from Siberian forest fires in summer 2012. Int. J. Rem. Sens. 35 (15), 5722–5741. http://dx.doi.org/10.1080/01431161.2014.945010.
Kundu, S., Kawamura, K., Andreae, T.W., Hoffer, A., Andreae, M.O., 2010. Molecular distributions of dicarboxylic acids, ketocarboxylic acids and α-dicarbonyls in biomass burning aerosols: implications for photochemical production and degradation in smoke layers. Atmos. Chem. Phys. 10 (5), 2209–2225. http://dx.doi.org/10.5194/acp-10-2209-2010.
Kuokka, S., Teinilä, K., Saarnio, K., Aurela, M., Sillanpää, M., Hillamo, R., Kerminen, V.-M., Pyy, K., Vartiainen, E., Kulmala, M., Skorokhod, A.I., Elansky, N.F., Belikov, I.B., 2007. Using a moving measurement platform for determining the chemical composition of atmospheric aerosols between Moscow and Vladivostok. Atmos. Chem. Phys. 7 (18), 4793–4805. http://dx.doi.org/10.5194/acp-7-4793-2007.
Lai, A.C., 2002. K.: particle deposition indoors: a review. Indoor Air 12 (4), 211–214. http://dx.doi.org/10.1046/j.0905-6947.2002.1r159a.x.
Lavoué, D., Liousse, C., Cachier, H., Stocks, B.J., Goldammer, J.G., 2000. Modeling of carbonaceous particles emitted by boreal and temperate wildfires at northern latitudes. J. Geophys. Res. Atmospheres 105 (D22), 26871–26890. http://dx.doi.org/10.1029/2000JD900180.
Lee, K.H., Kim, J.E., Kim, Y.J., Kim, J., von Hoyningen-Huene, W., 2005. Impact of the smoke aerosol from Russian forest fires on the atmospheric environment over Korea during May 2003. Atmos. Environ 39, 85–99. https://doi.org/10.1016/j.atmosenv.2004.09.032.
Levin, E.J.T., McMeeking, G.R., Carrico, C.M., Mack, L.E., Kreidenweis, S.M., Wold, C.E., Moosmüller, H., Arnott, W.P., Hao, W.M., Collett, J.L., et al., 2010. Biomass burning smoke aerosol properties measured during Fire Laboratory at Missoula Experiments (FLAME). J. Geophys. Res. Atmos. 115.
Li, C., Ma, Z., Chen, J., Wang, X., Ye, X., Wang, L., Yang, X., Kan, H., Donaldson, D.J., Mellouki, A., 2015. Evolution of biomass burning smoke particles in the dark. Atmos. Environ. 120, 244–252. http://dx.doi.org/10.1016/j.atmosenv.2015.09.003.
McKenzie, L.M., Hao, W.M., Richards, G.N., Ward, D.E., 1995. Measurement and modeling of air toxins from smoldering combustion of biomass. Environ. Sci. Technol. 29 (8), 2047–2054. http://dx.doi.org/10.1021/es00008a025.
McMeeking, G.R., Kreidenweis, S.M., Baker, S., Carrico, C.M., Chow, J.C., Collett, J.L., Hao, W.M., Holden, A.S., Kirchstetter, T.W., Malm, W.C., Moosmüller, H., Sullivan, A.P., Wold, C.E., 2009. Emissions of trace gases and aerosols during the open combustion of biomass in the laboratory. J. Geophys. Res. Atmos. 114 (D19), D19210,. http://dx.doi.org/10.1029/2009JD011836.
Morawska, L., (Jim) Zhang, J., 2002. combustion sources of particles. 1. Health relevance and source signatures. Chemosphere 49 (9), 1045–1058. http://dx.doi.org/10.1016/S0045-6535(02)00241-2.
Nguyen, Q.T., Skov, H., Sørensen, L.L., Jensen, B.J., Grube, A.G., Massling, A., Glasius, M., Nøjgaard, J.K., 2013. Source apportionment of particles at station Nord, North East Greenland during 2008–2010 using COPREM and PMF analysis. Atmos. Chem. Phys. 13 (1), 35–49. http://dx.doi.org/10.5194/acp-13-35-2013.
Nolte, C.G., Schauer, J.J., Cass, G.R., Simoneit, B.R.T., 2001. Highly polar organic compounds present in wood smoke and in the ambient atmosphere. Environ. Sci. Technol. 35 (10), 1912–1919. http://dx.doi.org/10.1021/es001420r.
Oros, D.R., Simoneit, B.R., 2001a. Identification and emission factors of molecular tracers in organic aerosols from biomass burning Part 2. Deciduous trees. Appl. Geochem. 16 (13), 1545–1565.
Oros, D.R., Simoneit, B.R.T., 2001b. Identification and emission factors of molecular tracers in organic aerosols from biomass burning Part 1. Temperate climate conifers. Appl. Geochem. 16 (13), 1513–1544. http://dx.doi.org/10.1016/S0883-2927(01)00021-X.
Paris, J.-D., Stohl, A., Nédélec, P., Arshinov, M.Y., Panchenko, M.V., Shmargunov, V.P., Law, K.S., Belan, B.D., Ciais, P., 2009. Wildfire smoke in the Siberian Arctic in summer: source characterization and plume evolution from airborne measurements. Atmos. Chem. Phys. 9 (23), 9315–9327. http://dx.doi.org/10.5194/acp-9-9315-2009.
Pashynska, V., Vermeylen, R., Vas, G., Maenhaut, W., Claeys, M., 2002. Development of a gas chromatographic/ion trap mass spectrometric method for the determination of levoglucosan and saccharidic compounds in atmospheric aerosols. Application to urban aerosols. J. Mass Spectrom. 37 (12), 1249–1257. http://dx.doi.org/10.1002/jms.391.
Peterson, M.R., Richards, M.H., 2002. Thermal-optical-transmittance analysis for organic, elemental, carbonate, total carbon, and OCX2 in PM2.5 by the EPA/NIOSH method-#83. In: Winegar, E.D., Tropp, R.J. (Eds.), Proceedings, Symposium on Air Quality Measurement Methods and Technology-2002. Air & Waste Management Association., Pittsburgh, PA [online] Available from. www.rti.org/sites/default/files/resources/OC-EC_Paper_83_3b.pdf.
Popovicheva, O.B., 2010. Combustion-Derived Carbonaceous Aerosols (Soot) in the Atmosphere: Water Interaction and Climate Effects. In: Agranovski, I. (Ed.), Aerosols - Science and Technology. Wiley-VCH Verlag GmbH & Co. KGaA, pp. 127–157.
Popovicheva, O.B., Kistler, M., Kireeva, E., Persiantseva, N., Timofeev, M., Kopeikin, V., Kasper-Giebl, A., 2014. Physicochemical characterization of smoke aerosol during large-scale wildfires: Extreme event of August 2010 in Moscow. Atmos. Environ. 96, 405–414. http://dx.doi.org/10.1016/j.atmosenv.2014.03.026.
Popovicheva, O.B., Kozlov, V.S., Engling, G., Diapouli, E., Persiantseva, N.M., Timofeev, M.A., Fan, T.-S., Saraga, D., Eleftheriadis, K., 2015. Small-scale study of siberian biomass burning: I. Smoke microstructure. Aerosol Air Qual. Res. 15 (1), 117–128. http://dx.doi.org/10.4209/aaqr.2014.09.0206.
Popovicheva, O.B., Engling, G., Diapouli, E., Saraga, D., Persiantseva, N.M., Timofeev, M.A., Kireeva, E.D., Shonia, N.K., Chen, S.H., Nguyen, D.L., Eleftheriadis, K., Lee, C.T., 2016a. Impact of smoke intensity on size-resolved aerosol composition and microstructure during the biomass burning season in Northwest Vietnam. Aerosol Air Qual. Res. 16 (11), 2635–2654. http://dx.doi.org/10.4209/aaqr.2015.07.0463.
Popovicheva, O.B., Persiantseva, N.M., Timofeev, M.A., Shonija, N.K., Kozlov, V.S., 2016b. Small-scale study of siberian biomass burning: II. Smoke hygroscopicity. Aerosol Air Qual. Res. 16 (7), 1558–1568. http://dx.doi.org/10.4209/aaqr.2015.11.0648.
Popovicheva, O.B., Shonija, N.K., Persiantseva, N., Timofeev, M., Diapouli, E., Eleftheriadis, K., Borgese, L., Nguyen, X.A., 2017. Aerosol pollutants during agricultural biomass burning: a case study in Ba Vi region in Hanoi, Vietnam. Aerosol Air Qual. Res. 17 (11), 2762–2779. http://dx.doi.org/10.4209/aaqr.2017.03.0111.
Puxbaum, H., Caseiro, A., Sánchez-Ochoa, A., Kasper-Giebl, A., Claeys, M., Gelencsér, A., Legrand, M., Preunkert, S., Pio, C., 2007. Levoglucosan levels at background sites in Europe for assessing the impact of biomass combustion on the European aerosol background. J. Geophys. Res. Atmos. 112 (D23), D23S05,. http://dx.doi.org/10.1029/2006JD008114.
Reid, J.S., Koppmann, R., Eck, T.F., Eleuterio, D.P., 2005. A review of biomass burning emissions part II: intensive physical properties of biomass burning particles. Atmos. Chem. Phys. 5 (3), 799–825. http://dx.doi.org/10.5194/acp-5-799-2005.
Samsonov, Y.N., Koutsenogii, K.P., Makarov, V.I., Ivanov, A.V., Ivanov, V.A., McRae, D.J., Conard, S.G., Baker, S.P., Ivanova, G.A., 2005. Particulate emissions from fires in central Siberian Scots pine forests. Can. J. For. Res. 35 (9), 2207–2217. http://dx.doi.org/10.1139/x05-199.
Samsonov, Y.N., Ivanov, V.A., McRae, D.J., Baker, S.P., 2012. Chemical and dispersal characteristics of particulate emissions from forest fires in Siberia. Int. J. Wildland Fire 21 (7), 818–827. http://dx.doi.org/10.1071/WF11038.
Schauer, J.J., Kleeman, M.J., Cass, G.R., Simoneit, B.R.T., 2001. Measurement of emissions from air pollution sources. 3. C1 − C29 organic compounds from fireplace combustion of wood. Environ. Sci. Technol. 35 (9), 1716–1728. http://dx.doi.org/10.

1021/es001331e.
Schmidl, C., Marr, I.L., Caseiro, A., Kotianová, P., Berner, A., Bauer, H., Kasper-Giebl, A., Puxbaum, H., 2008. Chemical characterisation of fine particle emissions from wood stove combustion of common woods growing in mid-European Alpine regions. Atmos. Environ. 42 (1), 126–141. http://dx.doi.org/10.1016/j.atmosenv.2007.09.028.
Simoneit, B.R.T., Schauer, J.J., Nolte, C.G., Oros, D.R., Elias, V.O., Fraser, M.P., Rogge, W.F., Cass, G.R., 1999. Levoglucosan, a tracer for cellulose in biomass burning and atmospheric particles. Atmos. Environ. 33 (2), 173–182. http://dx.doi.org/10.1016/S1352-2310(98)00145-9.
Simoneit, B.R.T., Rogge, W., Lang, Q., Jaffé, R., 2000. Molecular characterization of smoke from campfire burning of pine wood (Pinus elliottii). Chemosphere Global Change Sci. 2 (1), 107–122. http://dx.doi.org/10.1016/S1465-9972(99)00048-3.
Simoneit, B.R.T., Elias, V.O., Kobayashi, M., Kawamura, K., Rushdi, A.I., Medeiros, P.M., Rogge, W.F., Didyk, B.M., 2004. SugarsDominant water-soluble organic compounds in soils and characterization as tracers in atmospheric particulate matter. Environ. Sci. Technol. 38 (22), 5939–5949. http://dx.doi.org/10.1021/es0403099.
Stocks, B.J., Fosberg, M.A., Lynham, T.J., Mearns, L., Wotton, B.M., Yang, Q., Jin, J.-Z., Lawrence, K., Hartley, G.R., Mason, J.A., McKenney, D.W., 1998. Climate change and forest fire potential in Russian and Canadian boreal forests. Clim. Change 38, 1–13. https://doi.org/10.1023/A:1005306001055.
Tiitta, P., Leskinen, A., Hao, L., Yli-Pirilä, P., Kortelainen, M., Grigonyte, J., Tissari, J., Lamberg, H., Hartikainen, A., Kuuspalo, K., Kortelainen, A.-M., Virtanen, A., Lehtinen, K.E.J., Komppula, M., Pieber, S., Prévôt, A.S.H., Onasch, T.B., Worsnop, D.R., Czech, H., Zimmermann, R., Jokiniemi, J., Sippula, O., 2016. Transformation of logwood combustion emissions in a smog chamber: formation of secondary organic aerosol and changes in the primary organic aerosol upon daytime and nighttime aging. Atmos. Chem. Phys. 16 (20), 13251–13269. http://dx.doi.org/10.5194/acp-16-13251-2016.
Tolocka, M.P., Jang, M., Ginter, J.M., Cox, F.J., Kamens, R.M., Johnston, M.V., 2004. formation of Oligomers in secondary organic aerosol. Environ. Sci. Technol. 38 (5), 1428–1434. http://dx.doi.org/10.1021/es035030r.
Turpin, B.J., Lim, H.-J., 2001. Species contributions to PM2.5 mass concentrations: Revisiting common assumptions for estimating organic mass. Aerosol Sci. Technol. 35 (1), 602–610. http://dx.doi.org/10.1080/02786820119445.
Wang, G., Kawamura, K., Cheng, C., Li, J., Cao, J., Zhang, R., Zhang, T., Liu, S., Zhao, Z., 2012. Molecular distribution and stable carbon isotopic composition of dicarboxylic acids, ketocarboxylic acids, and α-dicarbonyls in size-resolved atmospheric particles from Xi'an city, China. Environ. Sci. Technol. 46 (9), 4783–4791. http://dx.doi.org/10.1021/es204322c.
Ward, D.E., Hardy, C.C., 1991. Smoke emissions from wildland fires. Environ. Int. 17 (2), 117–134. https://doi.org/10.1016/0160-4120(91)90095-8.
Ward, T.J., Hamilton, R.F., Dixon, R.W., Paulsen, M., Simpson, C.D., 2006. Characterization and evaluation of smoke tracers in PM: results from the 2003 Montana wildfire season. Atmos. Environ. 40 (36), 7005–7017. https://doi.org/10.1016/j.atmosenv.2006.06.034.
Warneke, C., Bahreini, R., Brioude, J., Brock, C.A., de Gouw, J.A., Fahey, D.W., Froyd, K.D., Holloway, J.S., Middlebrook, A., Miller, L., Montzka, S., Murphy, D.M., Peischl, J., Ryerson, T.B., Schwarz, J.P., Spackman, J.R., Veres, P., 2009. Biomass burning in Siberia and Kazakhstan as an important source for haze over the alaskan arctic in april 2008. Geophys. Res. Lett. 36 (2), L02813. http://dx.doi.org/10.1029/2008GL036194.
Zepp, R.G., Faust, B.C., Hoigne, J., 1992. Hydroxyl radical formation in aqueous reactions (pH 3-8) of iron(II) with hydrogen peroxide: the photo-Fenton reaction. Environ. Sci. Technol. 26 (2), 313–319. http://dx.doi.org/10.1021/es00026a011.